Experimental Matrix Isolation Study and Quantum-Mechanics-Based Normal-Coordinate Analysis of the Anharmonic Infrared Spectrum of Picolinic Acid *N*-Oxide

Krystyna Szczepaniak,[†] Willis B. Person,*[,†] and Dušan Hadži[‡]

Department of Chemistry, University of Florida, P O Box 117200, Gainesville, Florida 32611, and the National Institute of Chemistry, Hajdrihova 19, SI-1000, Ljubljana, Slovenia

Received: March 11, 2005

This work is, according to our knowledge, the first experimental matrix isolation study of a molecular system with a very short and strong intramolecular OH···O hydrogen bond. It also includes a satisfying interpretation of its entire infrared spectrum. The interpretation relies on the calculation at the DFT/B3LYP/6-31G(d,p) level of the harmonic spectrum and of the anharmonic relaxed potential energy for the stretching motion of the hydrogen-bonded proton, used with our recently modified quantum-mechanics-based normal-coordinate analysis. An important observation about the anharmonic spectrum obtained from this procedure is that the OH stretch coordinate contributes to several normal modes, mixing extensively with other in-plane internal coordinates, in particular OH-bending and C═O-stretching. The two intense normal modes with the largest contributions from the OH-stretching coordinate to the potential energy distribution and to the intensity are located near 1700 and 1500 cm^{-1}. A calculated anharmonic spectrum obtained from this procedure agrees with the experimental spectrum (frequencies and intensity distribution), within the limits of the estimated uncertainties for the calculation and experiment, allowing the interpretation of the latter. The agreement for the frequencies is about 1−3%. The anharmonic spectrum calculated using the anharmonic keyword in Gaussian 03w is not in satisfactory agreement with experiment insofar as the OH-stretching mode is concerned.

Introduction

Picolinic acid *N*-oxide (PANO, Figure 1) is a relatively simple representative of molecular systems with a very short and strong intramolecular OH···O hydrogen bond. The potential energy surface for such a system, in particular the potential energy for the hydrogen-bonded proton motion, is the vital point of interest. The vibrational spectrum should, in principle, provide information about this potential. However, a correct interpretation of the spectrum is a prerequisite for this information to be reliable.

In recent years, there have been several studies of the structure and the infrared spectra of PANO and related systems.[1−5] The most recent X-ray diffraction study of PANO[3] indicates that the O1···O2 distance is only 2.428 Å. Experimental infrared spectra of crystalline solids and solutions in various solvents[1,4,5] show an extremely flat and broad absorption with very low intensity at maximum in the region from 2300 to 2800 cm^{-1} which was attributed by some authors[4] to the absorption by the fundamental OH stretching mode, ν(OHs), and by others to the to the $0 \rightarrow 2$ transition.[5] The latter authors[5] assigned ν(OHs) to the broader absorption near 1000 cm^{-1}. However, closer examination of infrared spectra of solid PANO[1,5] and results from inelastic neutron scattering studies of PANO[6] suggest that the band near 1000 cm^{-1} is almost certainly related to the out-of-plane COH bending motion. The authors in ref 1 assigned ν(OHs) in spectra of PANO in the crystalline solid and in solutions predominantly to the broad absorption around 1500 cm^{-1}.

Identification of absorption due to the OH-stretching vibration in systems with short (less than 2.50 Å for the O···O distance) intramolecular hydrogen bonds is often controversial. In the most widely investigated group of such compounds (β-diketones in enolic form) Tayyari et al.[7] assigned ν(OHs) for diketones with O···O distance < 2.50 Å to a very broad absorption with low peak intensity near 2600 cm^{-1}. This assignment was accepted by Bertolasi et al.,[8] but disputed by Emsley et al.;[9] the latter authors attributed the broad absorption near 2600 cm^{-1} to overtones and suggested that ν(OHs) absorption should be located near 1500 cm^{-1}.

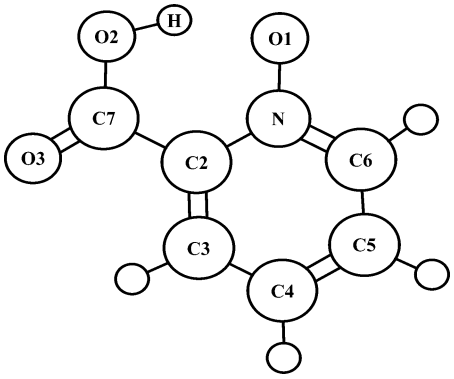

Figure 1. Calculated structure of PANO and numbering of atoms. Calculation at DFT/B3LYP/6-31G(d,p) level leads to planar geometry for PANO in vacuo and in the field ($\epsilon = 1.6$).

The experimental spectra of PANO[1,5] are severely different from the spectra obtained from various quantum-mechanical calculations at the harmonic approximation. In particular, calculations at DFT/B3LYP/6-311++G(3df,3pd) level locate ν_{ha}(OHs) at 2977 cm^{-1}.[10] The experimental spectra[1,5] are more consistent with the anharmonic spectrum of PANO (in vacuo) calculated by Stare and Mavri[11] using a two-dimensional approach for the O2−H and O2···O1 internal coordinates, which leads to ν_{anh}(OH s) at about 1733 cm^{-1}, or with the anharmonic

* Corresponding author. E-mail: person@chem.ufl.edu.
[†] University of Florida.
[‡] National Institute of Chemistry, Slovenia.

10.1021/jp058089o CCC: $30.25
Published on Web 07/08/2005

spectrum calculated by the CPMD method for PANO in the crystal, which predicts ν_{anh}(OHs) at 1407 cm^{-1}.[12] Yet, even if these values of ν_{anh}(OHs) are used, a complete interpretation of the entire experimental spectrum is still a challenge.

One of the problems with the interpretation of the results of studies of solutions and solid is the effect of the solvent or crystal environment on the geometry and the spectrum of PANO, as indicated clearly in the recent work by Panek, Stare, and Hadži.[12] This problem can be avoided by studying PANO isolated in a relatively inert Ar matrix. It can be expected that the spectrum of such an isolated molecule will be little disturbed by the environment, and thus be more suitable for comparison with the calculated spectrum.

Another major problem is the possibility of interaction between the lower-frequency anharmonic OH-stretching coordinate and the in-plane OH-bending coordinate (linked to the band near 1570 cm^{-1}). Such interaction was emphasized in the recent extensive study by Stare and Balint-Kurti.[10] Interaction of the anharmonic OH stretching coordinate with other internal coordinates, especially with the C═O stretching, could also occur. As will be shown below, such interactions play a crucial role in determining the appearance of the infrared spectrum. Similar effects were observed previously in studies of the hydrogen maleate ion,[13] a classical example of a molecule with a short intramolecular hydrogen bond for which a normal coordinate analysis was performed using the OH proton potential function obtained from an ab initio 4-31G calculation.[13]

An advantage of studying PANO, compared to diketones, lies in its asymmetric potential—one does not have to consider possible effects of proton tunneling. PANO is also an attractive candidate for study because of availability of experimental data (although, only in condensed phases) and a possibility of the model calculations of potential energy surface. The effect of the environment on geometry,[12] the large differences between the spectra of solid PANO and of its solutions,[1,5] and, presented in this work, the spectrum of PANO isolated in Ar matrix are all of considerable interest.

In contrast to quandaries apparent for systems with very short hydrogen bonds, the spectrum of the prototype for intramolecular hydrogen bonds, malonaldehyde, a low barrier system with a longer, highly symmetrical bond seems to be much better understood,[14−17] although a mixing of the OH stretch with other internal coordinates (CH-stretching, as well as with the combination modes) is important.[16,17]

The aims of the present work are as follows: To obtain the experimental infrared spectrum (frequencies and integrated intensities) of PANO isolated in an Ar matrix and to interpret this spectrum on the basis of calculation (at the DFT/B3LYP/6-31G(d,p) level[18] using Gaussian 98w (g98w)[19] and Gaussian 03w (g03w) software[20]) of the potential energy (SCAN[21] and RELAXED[22]) for the hydrogen-bonded proton-stretching internal coordinate, and of the anharmonic spectrum utilizing first, g03w software[20] and then our specially developed procedure for a quantum-mechanics-based normal-coordinate-analysis with the anharmonic frequency ν_{anh}(OHs) from the calculated relaxed potential.

Methods

Experimental Procedure. Infrared spectra were recorded on a Nicolet FTIR spectrometer (model 740). A closed-cycle helium cryostat model DE-202 (from APD Cryogenic, Inc.), cooling to about 10 K, was used. A sample of crystalline PANO was placed inside the cryostat in a small wire-wrapped glass container heated resistively to a temperature of about 60 C, causing it to sublime. The resulting PANO vapor mixed with high purity Ar gas introduced through a needle valve into the cryostat chamber and the gaseous mixture deposited onto the cold CsI window to form the matrix. The matrix ratio (Ar:PANO) was greater than 10 000:1 (estimated utilizing experimental integrated absorbance of chosen bands, the corresponding calculated molar absorption coefficients and the optical path length obtained from the interference fringes[23]).

To be sure that the sample had not decomposed during heating, the solid PANO remaining in the glass container after matrix experiment was removed and put into a KBr pellet. The IR spectrum of this pellet was recorded and found to be identical with the spectrum of unheated PANO in KBr, confirming that no decomposition had occurred during heating of the sample in matrix experiment. Other details of the experiment have been described in our previous work[24−26] and references therein.

The experimental spectra were transferred from the Nicolet to a PC to be analyzed using grams software.[27] As described in more detail in ref 24, this software was used to measure the integrated absorbance of each observed band (area under the band contour which is proportional to the intensity), to separate overlapping bands in some spectral regions, and to estimate the relative intensities of each component in such overlapping bands and, finally, to perform baseline correction to obtain the final spectra shown in the following figures with a horizontal baseline at zero. The uncertainty of the experimental frequencies of the bands is about 1 cm^{-1}. The uncertainty of measurement of the integrated absorbances of the nonoverlapped and relatively intense bands is on the order of 10−20% (primarily caused by uncertainty in the baseline and in defining the region of the integration). The uncertainty of measurement of the integrated absorbance of the components of the overlapping bands and of the very weak bands is larger.

The experimental integrated absorbance measured for each band of the spectrum of matrix sample was normalized by multiplication by a constant factor to obtain values of the absolute molar absorption coefficient (in km/mol). This procedure has been described in more detail in ref 24. The normalization factor accounts for the reciprocal product of the thickness of the sample (matrix deposit) and concentration. This factor is obtained by supposing that the integrated absorption coefficient A_s of the chosen distinct and nonoverlapped band (at 853 cm^{-1}) in the experimental spectrum is equal to the calculated molar absorption coefficient (24 km/mol) of the corresponding mode (see later discussion).

Calculation Procedures. The calculations at the B3LYP/6-31G(d,p)[18] level were carried out using g98w[19] and g03w[20] software on a Dell Dimension XPS model T700r or model 8300 PC. Calculations have been performed to obtain the optimized structure, the one-dimensional single-point (SCAN[21] and RELAXED[22]) potential energy curves for the hydrogen-bonded proton stretching coordinate, the force field, the atomic polar tensors and infrared intensities and thus the infrared spectra at harmonic and anharmonic approximations using various procedures described in the following text. Other calculations using the Volume and SCRF keywords[21,22] were made to obtain the infrared spectrum of PANO in a field with dielectric constant $\epsilon = 1.6$ [28] (modeling the field in Ar matrix). The calculated infrared spectra were simulated[24] using grams software[27] and analyzed using animol[29] and our normal coordinate program xtrapack.[30]

An important step in the analysis of the results of calculations is transformation of the force constants in Cartesian coordinates obtained from Gaussian to the force constants in the nonredun-

TABLE 1: Symmetry Coordinates of PANO

name used in tables	definition[a]
	In-Plane Coordinates
1 O2H s	δr_{O2H}
2 C2C3 s	δr_{C2C3}
3 C3C4 s	δr_{C3C4}
4 C4C5 s	δr_{C4C5}
5 C5C6 s	δr_{C5C6}
6 NC6 s	δr_{NC6}
7 NO1 s	δr_{NO1}
8 C7C2 s	δr_{C7C2}
9 C7−O2 s	δr_{C7O2}
10 NC2 s	δr_{NC2}
11 C7═O3 s	$\delta r_{C7=O3}$
12 C6H s	δr_{C6H}
13 C5H s	δr_{C5H}
14 C4H s	δr_{C4H}
15 C3H s	δr_{C3H}
16 Ri def1	$n_1(\delta\beta_{C5C6N} - \delta\beta_{C6NC2} + \delta\beta_{NC2C3} + \delta\beta_{C2C3C4} + \delta\beta_{C3C4C5} - \delta\beta_{C4C5C6})$
17 Ri def2	$n_2(2\delta\beta_{C5C6N} - \delta\beta_{C6NC2} - \delta\beta_{NC2C3} + 2\delta\beta_{C2C3C4} - \delta\beta_{C3C4C5} - \delta\beta_{C4C5C6})$
18 Ri def3	$n_3(\delta\beta_{C6NC2} - \delta\beta_{NC2C3} + \delta\beta_{C3C4C5} - \delta\beta_{C4C5C6})$
19 C3H be	$n_4(\delta\beta_{HC3C2} - \delta\beta_{HC3C4})$
20 C4H be	$n_4(\delta\beta_{HC4C3} - \delta\beta_{HC4C5})$
21 C5H be	$n_4(\delta\beta_{HC5C6} - \delta\beta_{HC5C4})$
22 C6H be	$n_4(\delta\beta_{HC6N} - \delta\beta_{HC6C5})$
23 NO1 be	$n_4(\delta\beta_{C6NO1} - \delta\beta_{C2NO1})$
24 C2C7 be	$n_4(\delta\beta_{NC2C7} - \delta\beta_{C3C2C7})$
25 C2C7O2 be	$\delta\beta_{C2C7O2}$
26 O3C7be	$n_4(\delta\beta_{C2C7=O3} - \delta\beta_{O2C7=O3})$
27 HO2C7 be	$\delta\beta_{C7O2H}$
	Out-of-Plane Coordinates
28 oRi def1	$n_1(-\tau_{C5C6NC2} + \tau_{C6NC2C3} - \tau_{NC2C3C4} + \tau_{C2C3C4C5} - \tau_{C3C4C5C6} + \tau_{C4C5C6N})$
29 oRi def2	$n_3(\tau_{C5C6NC2} - \tau_{NC2C3C4} + \tau_{C2C3C4C5} - \tau_{C4C5C6N})$
30 oRi def3	$n_2(-\tau_{C5C6NC2} + 2\tau_{C6NC2C3} - \tau_{NC2C3C4} - \tau_{C2C3C4C5} + 2\tau_{C3C5C5C6} - \tau_{C4C5C6N})$
31 oNO1 w	$\gamma_{O1NC2C6}$
32 oC3H w	$\gamma_{HC3C4C2}$
33 oC4H w	$\gamma_{HC4C5C3}$
34 oC5H w	$\gamma_{HC5C4C6}$
35 oC6H w	γ_{HC6NC5}
36 oCC2 w	$n_4(\tau_{C7C2C3C4} - \tau_{C7C2NC6})$
37 oOCO tw	$n_4(\tau_{O3=C7C2C3} + \tau_{O2C7C2C3})$
38 oOCO w	$n_4(\tau_{O3=C7C2C3} - \tau_{O2C7C2C3})$
39 oHOC7 t	$\tau_{HO2C7=O}$

[a] δr_{ij} is an increase in the distance between the atoms i and j; $\delta\beta_{ijk}$ is an increase in the angle formed by atoms i and k with the central atom j; γ_{ijkl} is a positive wagging of atom i attached to atom j moving perpendicular to the plane defined by atoms j, k, and l; τ_{ijkl} designates the torsion about the jk bond. Normalization factors: $n_1 = 6^{-1/2}$, $n_2 = 12^{-1/2}$, $n_3 = 4^{-1/2}$, $n_4 = 2^{-1/2}$

dant internal symmetry coordinates (given in Table 1), utilizing the familiar definitions given by Wilson, Decius, and Cross[31a] or Califano.[31b] To carry out a normal coordinate analysis and describe normal modes in terms of the nonredundant internal symmetry coordinates program xtrapack[30] was used. The output from xtrapack includes not only the harmonic frequencies and infrared intensities of the normal modes, but also the potential energy distributions (PEDs),[32,24,25] intensity distributions (IDs),[33,24] and the force constants in the internal symmetry coordinates.

An important difference in the xtrapack output from that of Gaussian is that the interpretation of the normal mode and its infrared intensity is given in terms of contributions from symmetry displacement coordinates instead of Cartesian displacement coordinates. We expect some transferability of properties of internal coordinates from one molecule to another.

Another important advantage of the xtrapack program is that it allows changing selected elements of force constant matrix. This possibility of the xtrapack program was utilized in calculation of the anharmonic spectrum. To obtain this spectrum the force constant matrix from g98w calculation was modified by replacing the harmonic values calculated for the diagonal element corresponding to the OH-stretching internal coordinate and the off-diagonal elements corresponding to the interaction constants of the OH stretching internal coordinate with all other symmetry coordinates by the values estimated for the anharmonic force constants. The values for the anharmonic force constants were derived from the anharmonic frequency ν_{anh}(OHs) based on the relaxed anharmonic potential for the OH-stretching coordinate (see discussion in the following sections).

Experimental Results and Discussion

Experimental Spectrum of PANO Isolated in an Ar Matrix. The experimental spectrum recorded in the region between 4000 and 550 cm^{-1} for PANO isolated in an Ar matrix at about 10 K is shown in Figure 2. The top trace shows the original unprocessed spectrum as recorded directly by the instrument. The continuously decreasing background is due to uncompensated scattering by the matrix (solid Ar) film. On this background we may see the superimposed interference fringes produced by the passage of the light through the thin film from a matrix deposit.[23] The bottom trace in Figure 2 is the spectrum of the same matrix after subtracting the background due to the scattering and to the interference fringes. Bands known to be due to absorption by monomeric H_2O impurity in the Ar matrix (at 3776, 3756, and 3711 cm^{-1} and at 1623, 1607, and 1572

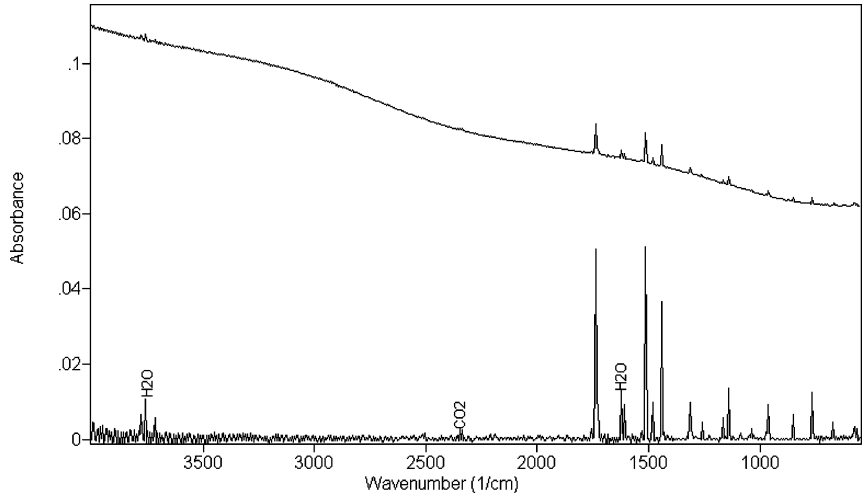

Figure 2. Experimental infrared spectrum of PANO isolated in Ar matrix at about 10 K. Top trace: the original spectrum as recorded on the Nicolet spectrometer; bottom trace-spectrum of the same matrix after subtracting the background due to the scattering and to the interference fringes. "H2O" and "CO2" indicate bands of the monomeric H_2O and CO_2 impurities in the matrix, respectively.

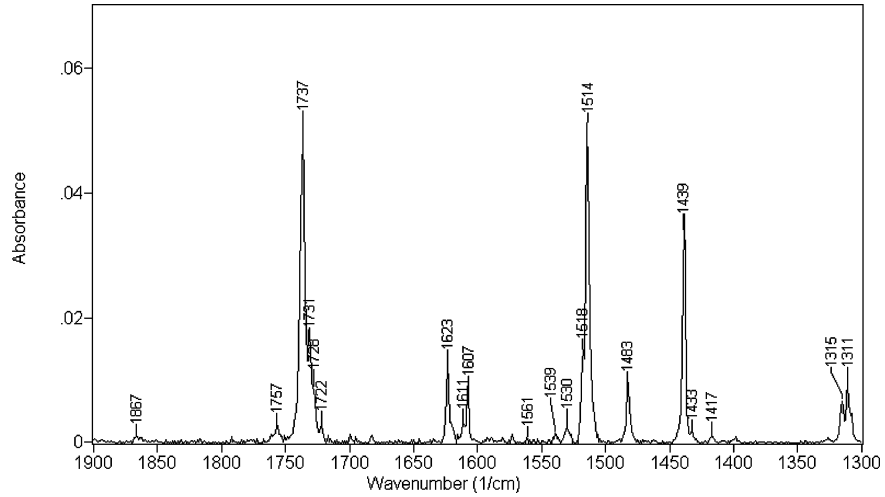

Figure 3. Infrared spectrum of PANO isolated in Ar matrix shown in the expanded scale in the region from 1900 to 1300 cm^{-1}.

cm^{-1}) are marked in the figure by "H2O". There is no indication (i.e., no new absorption bands) that the water molecules are involved in any hydrogen bonding with PANO. The trace bands at 2345 and 2339 cm^{-1} (marked by "CO2") are due to the CO_2 impurities in the matrix.

The most important observation from examination of the spectra shown in Figure 2 is that no intense absorption is observed in the region above 1737 cm^{-1}. Only very weak features, barely distinguishable from the noise, can be recognized, after a large expansion of the absorbance scale, between 3600 and 1740 cm^{-1}. These are most likely due to combination and overtone bands of various low-frequency vibrations rather than to a strong OH stretch fundamental absorption band.

The most intense absorption bands in this survey spectrum are found at 1737, 1514, and 1439 cm^{-1}. All other absorption, including those bands located below 1400 cm^{-1}, is much less intense.

Although all bands in the survey spectrum shown in Figure 2 appear to be very narrow, closer examination after the frequency scale is expanded shows that many of them consist of several components. To present a better view of details of the multicomponent structure of the absorption bands three regions of this spectrum are shown in Figures 3−5 with expanded frequency and intensity scales.

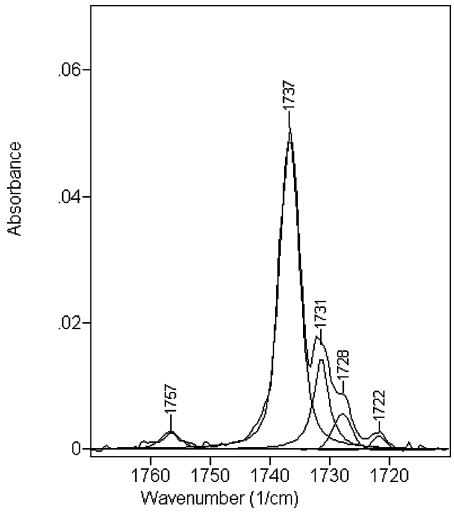

Figure 4. Separation into components (performed using Curve Fit procedure of Grams software) of the spectrum of PANO isolated in Ar matrix (region 1770−1710 cm^{-1}).

Figure 3 shows the spectral region between 1900 and 1300 cm^{-1}. As can be seen there, several subbands or satellites are visible in the vicinity of the more intense bands in several parts

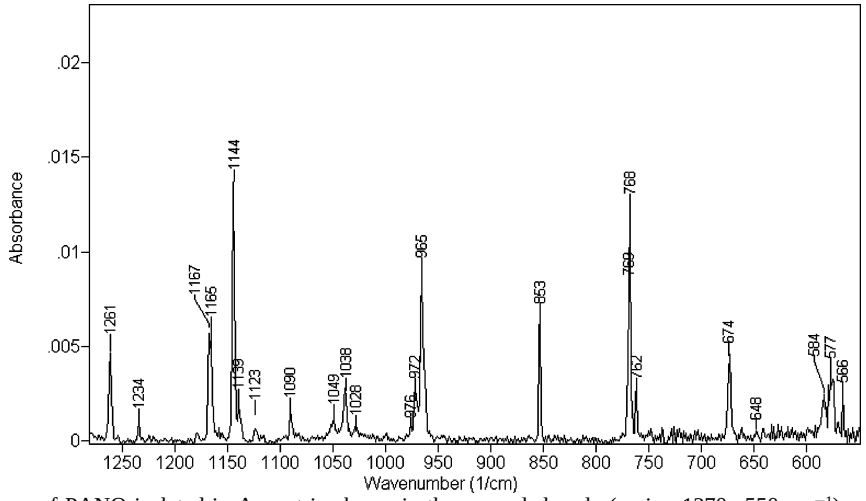

Figure 5. Infrared spectrum of PANO isolated in Ar matrix shown in the expanded scale (region 1270−550 cm^{-1}).

of the spectrum. The separation of such multicomponent absorption bands was done using Curve Fit procedure from the grams software.[27] Figure 4 shows an example of such separation for the absorption in the region near 1700 cm^{-1}.

Figure 5 shows the spectral region between 1300 and 550 cm^{-1}. The intensity of absorption in this region is much lower than that in Figure 3. To see these weak bands more clearly the absorbance scale is expanded from that shown in Figure 3 by a factor of 3. As seen in Figure 5, one or more subbands with very close frequencies appear again in several parts of the spectrum instead of a single band (e.g., near 1167, 1144, 965, 768, and 577 cm^{-1}). These subbands were separated using the Curve Fit procedure of grams.

The values of frequencies and integrated intensities corresponding to the experimental spectrum shown in Figures 3−5 (after decomposition of overlapping bands, in the regions where they occur) are collected in Table 2 together with the preliminary assignment. The final assignment is proposed and justified in the following sections of this paper.

Several possible explanations for the appearance of multicomponent bands in the infrared spectrum of PANO are suggested in Table 2. They are as follows: (a) Fermi resonance[34] between the strong fundamental mode and weaker overtone and/or combination bands with close frequencies; (b) site splitting resulting from the slightly different local environments of molecules in the matrix;[35] (c) absorption by fundamental modes with very close frequencies.

Comparison of the Experimental Spectrum with the Calculated Harmonic Spectrum. The experimental infrared spectrum of PANO isolated in an Ar matrix (upper trace) is compared in Figure 6 with the simulated spectrum of isolated PANO in vacuo (lower trace) calculated at the harmonic approximation and with the simulated harmonic spectrum of PANO in a dielectric field with dielectric constant $\epsilon = 1.6$ (middle trace). As seen, the main difference between the calculated and experimental spectra is the appearance in the former of an intense band at 2991 cm^{-1} for PANO in vacuo and at 2917 cm^{-1} for PANO in the field while in the experimental spectrum no intense band is found anywhere near this region.

The obvious explanation for the absence in the experimental spectrum of an intense band above 1737 cm^{-1} is that the OH stretching motion is highly anharmonic and the absorption band associated with it is shifted to lower frequency.[11,12] The spectral patterns in the region below 2000 cm^{-1} in both calculated spectra are almost identical and the frequencies are fairly similar to those in the experimental spectrum. All frequencies, intensities, and descriptions of the normal modes in these calculated

TABLE 2: Experimental Frequencies, Integrated Intensities, and Preliminary Assignment of Bands in the Spectrum of PANO Isolated in an Ar Matrix

band no.	ν_a (cm^{-1})	A_b (km/mol)		preliminary assignment[c]
1	1989[d]	10[d]		1144 + 762
2	1867[d]	10[d]		1311 + 566 or fundamental
3	1757	22	}	FR (1165 + 584)
4	1737	514		fundamental
5	1732	109	720	MS or FR (566 + 1165)
6	1728	56		FR (1144 + 584)
7	1722	19	}	FR (1144 + 577)
8	1698	10[d]		1311 + 396
9	1682	10[d]		2 × 853
10	1611[d]	10[d]		fundamental
11	1561[d]	3[d]		fundamental
12	1539	20	}	FR (2 × 769)
13	1530	38		FR (2 × 768)
14	1518	117	525	FR (2 × 762
15	**1514**	**325**		fundamental
16	1509	25	}	MS
17	1483	69		fundamental
18	**1439**	**217**	}	fundamental
19	1433	4	228	FR (768 + 674)
20	1417	7	}	FR (853 + 566)
21	1315	28	} 120	MS or FR (674 + 641)
22	**1311**	**92**		fundamental
23	1261	32		fundamental
24	1220	2[d]		fundamental
25	1167	15	}	MS
26	**1165**	**40**	55	fundamental
27	1158	1[d]		fundamental
28	**1144**	**60**	}	fundamental
29	1139	10	70	FR (577 + 566)
30	1090	7	}	fundamental
31	1049	6	}	FR
32	**1038**	**20**	26	fundamental
33	1000[d]	2[d]		combination
34	976	2[d]		fundamental
35	972	9		fundamental
36	965	83		fundamental
37	877[d]	1[d]		fundamental
38	853	24		fundamental
39	769	38		fundamental
40	768	19		fundamental
41	762	9		fundamental
42	674	23		fundamental
43	648[d]	2[d]		fundamental
44	584	20	}	FR
45	**577**	**27**	47	fundamental
46	566	8		fundamental

[a] In a group of overlapped bands the most intense is in bold. [b] Normalized integrated intensity (see text). For the overlapped bands (marked by braces) a sum of components intensities is given. [c] FR = Fermi resonance; MS = matrix splitting. [d] Frequency and/or intensity not certain.

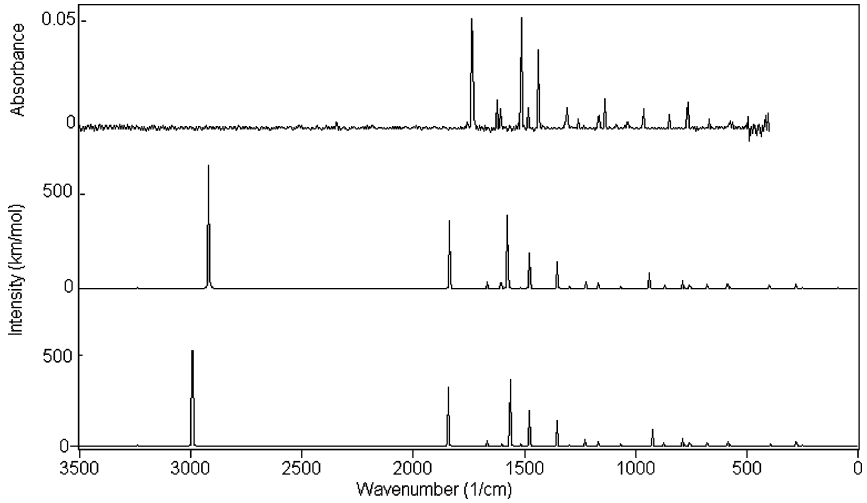

Figure 6. Comparison of the experimental spectrum of PANO isolated in Ar matrix (top trace) with the spectrum calculated at DFT/B3LYP/6-31G(d,p) level at harmonic approximation of PANO in vacuo (bottom trace) and of PANO in the field with dielectric constant $\epsilon = 1.6$ (middle trace).

harmonic spectra are given in the following tables, where they are compared with corresponding data calculated at anharmonic approximation and with the experimental data.

Anharmonic Potential for Stretching the OH Bond in PANO

SCAN Potential of PANO in Vacuo. The simplest way to obtain the one-dimensional potential energy curve as a function of the internal O−H stretching displacement coordinate is to use the scan procedure of Gaussian.[21,22] In this procedure the increase in energy from equilibrium ($E - E_e$) for the system is calculated point-by-point, changing the value of R(OH) by small increments (0.05 Å) from the calculated equilibrium value, R_e-(OH). Multiplication of the displacement from equilibrium by the square root of the reduced mass converts to the mass-weighted internal displacement coordinate $q(\mathrm{OH}) = \mu^{1/2}$ [R(OH) $- R_e$(OH)].

The points calculated at the DFT/B3LYP/6-31G(d,p) level for PANO in vacuo are fit by the light line shown in Figure 7. For values of the energy difference ($E - E_e$) varying from 0 to 5000 cm^{-1} (which includes the fundamental or v = 0 → v = 1 transition), these points can be fit by a fourth order polynomial. Under the assumption that the dimensionless normal coordinate (Q/γ, in the notation of Wilson, Decius, and Cross[31a]) for this motion is just equal to q, the mass-weighted internal OH displacement coordinate, we may use this fourth-order polynomial as the perturbation in the Somorjai and Hornig perturbation treatment[36,37] to solve the one-dimensional time-independent Schrödinger equation to obtain the anharmonic frequency for the (v = 0 → v = 1) transition, ν_{anh}(OHs), and the vibrationally averaged OH distance in the v = 0 vibrational state $\langle R_0(\mathrm{OH})\rangle$. The obtained values are

$$\nu_{anh}(\mathrm{OHs}) = 2420\ \mathrm{cm}^{-1} \quad \text{and} \quad \langle R_0(\mathrm{OH})\rangle = 1.0387\ \text{Å}$$

This anharmonic frequency is much higher than values estimated using two-dimensional approximations by Stare and Mavri[11] from different fitting schemes (ν_{anh}(OHs) = 2019, 1750, 1733, or 1723 cm^{-1}). It is certainly too high to explain the experimental spectrum, since no intense absorption is found in the region near 2400 cm^{-1}.

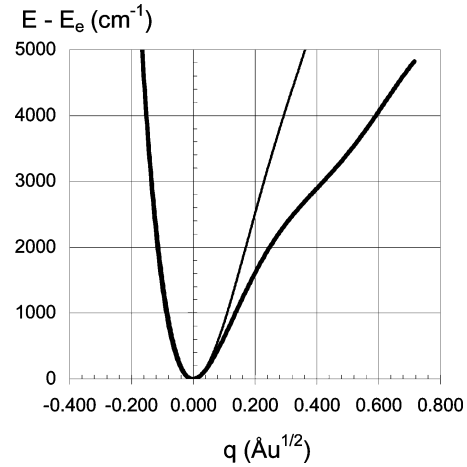

Figure 7. Comparison of the potential energy curves for OH stretching symmetry coordinate of PANO in vacuo calculated at DFT/B3LYP/6-31G(d,p) level (point by point calculation): light line, potential calculated using Scan procedure; heavy line, relaxed potential.

Relaxed Potential of PANO in Vacuo. An alternative way to calculate the anharmonic one-dimensional potential energy as a function of R(OH) is to use the relaxed potential energy calculation in redundant internal coordinates (partial optimization method described in ref 22a, p 148). In this point-by-point procedure constrained-geometry optimization is performed at each value of the OH distance to obtain the new energy and new geometry for a molecule at the stationary point for each new value of the OH distance. These points fit the heavy line in Figure 7 showing the "relaxed potential energy curve" calculated at the DFT/B3LYP/6-31G(d,p) level for PANO in vacuo.

For ($E - E_e$) values from 0 to 5000 cm^{-1}, including the fundamental v = 0 → v = 1 transition, this potential also can be fit by another fourth order polynomial. The perturbation solution of the one-dimensional time-independent Schrödinger equation using this relaxed potential in the Somorjai−Hornig procedure[36,37] leads to an anharmonic frequency of the (v = 0 → v = 1) transition, ν_{anh}(OHs) and to a vibrationally averaged OH distance in the v = 0 vibrational state $\langle R_0(\mathrm{OH})\rangle$. Because the fit of the fourth-order polynomial to the calculated relaxed potential curve is not precise, it is estimated that the value of

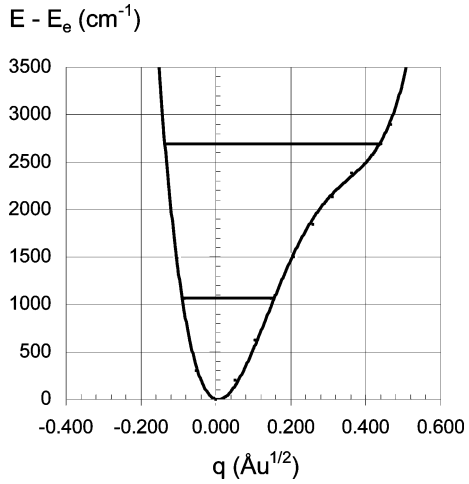

Figure 8. Relaxed potential energy curve for OH stretching symmetry coordinate of PANO in the field with dielectric constant $\epsilon = 1.6$ calculated at DFT/B3LYP/6-31G(d,p) level. The vibrational energy levels v = 0 and v = 1 are shown by the horizontal lines.

the anharmonic frequency from this relaxed potential is more accurately given as

$$\nu_{anh}(\mathrm{OHs}) = 1750 \pm 75\ \mathrm{cm}^{-1} \quad \text{and}$$
$$\langle R_0(\mathrm{OH})\rangle = 1.056_7 \pm 0.005\ \text{Å}$$

This estimate of ν_{anh}(OHs) and $\langle R_0(\mathrm{OH})\rangle$ agrees within its uncertainty with the values obtained by Stare and Mavri[11] (ν_{anh}(OHs) at about 1733 cm^{-1} and $\langle R_0(\mathrm{OH})\rangle = 1.062$ Å) in their two-dimensional calculation, suggesting that the "relaxation" of geometry that occurs after the length of the OH bond is increased allows the O1···O2 distance to adjust in the same way that occurs in the two-dimensional calculation. At any rate, it seems to justify the use of the one-dimensional relaxed potential energy curve as the perturbation function for use with the Somorjai−Hornig procedure to estimate anharmonicity.

Relaxed Potential of PANO in a Dielectric Field with Dielectric Constant $\epsilon = 1.6$. It is now appropriate to investigate the effect of a dielectric field on the shape of the relaxed potential energy function for the OH stretching vibration in PANO. The result of calculations similar to that described above of the relaxed potential energy for PANO in a field with dielectric constant $\epsilon = 1.6$ (corresponding to PANO in an Ar matrix[28]) is shown in Figure 8. This potential curve is similar in shape to the relaxed potential shown in Figure 7 for PANO in vacuo, but slightly broader, with its shoulder at a lower energy. The Somorjai−Hornig[36,37]perturbation calculation with this potential leads to

$$\nu_{anh}(\mathrm{OHs}) = 1625 \pm 75\ \mathrm{cm}^{-1} \quad \text{with}$$
$$\langle R_0(\mathrm{OH})\rangle = 1.066_4 \pm 0.005\ \text{Å}$$

Anharmonic energy levels calculated for the v = 0 and v = 1 states are shown in Figure 8 by the horizontal lines.

The value of $\langle R_0(\mathrm{OH})\rangle$ ($= 1.066_4$ Å) is much larger than the equilibrium distance for PANO in the dielectric field with $\epsilon = 1.6$ ($R_e(\mathrm{OH}) = 1.013_7$ Å), but it is close to the experimental value for crystalline PANO from neutron diffraction studies[38] (R_{ex}(OH) is 1.069 Å at 295 K or 1.091 Å at 15 K) and to the value calculated for the anharmonic OH oscillator of PANO *in vacuo* by Stare and Mavri[11] (1.062 Å) and by Panek, Stare, and Hadži[12] for PANO monomer (from 1.046 to 1.068 Å, depending on the method of calculation).

Anharmonic Spectrum of PANO

Anharmonic Spectrum from Gaussian 03w for PANO in Vacuo. The first method we have investigated to obtain the full anharmonic spectrum of PANO (in vacuo) is the anharmonic option provided in the g03w software (ref 22b, pp 87, 91).

Table 3 lists the calculated harmonic frequencies, the intensities, and the description of normal modes (in terms of the internal symmetry coordinates given in Table 1). To simplify Table 3, in the description of normal modes by the symmetry coordinates, the values of PEDs and IDs are omitted because they are almost identical to the corresponding PEDs and IDs for PANO in the field with $\epsilon = 1.6$ given in the tables at the end of this work. The anharmonic frequencies (from g03w anharmonic) for PANO in vacuo, ν_{anhG03}, are listed in column five of the table. In column six the ratio of the anharmonic to harmonic frequency, ν_{anh}/ν_{ha}, is given for each normal mode to indicate the variation of this ratio for different normal modes. Unfortunately, the anharmonic option in g03w does not provide intensities for the anharmonic spectrum. In the last two columns the experimental frequencies, ν_{exp}, and intensities, A_{exp}, of PANO isolated in an Ar matrix are given for comparison.

The most disappointing feature in the calculated anharmonic spectrum in Table 3 is the prediction of the OH-stretching mode at 2421 cm^{-1}, which is certainly not consistent with the experimental spectrum, unless this calculated normal mode has very low intensity (which is very unlikely[39]) and it is not detected experimentally. Presumably, the explanation for the failure of the g03w procedure to calculate correctly the frequency of the strongly anharmonic OH− stretching mode in PANO is its failure to allow for relaxation of the geometry. This explanation is suggested by the fact that the anharmonic frequency ν_{anh}(OHs) = 2421 cm^{-1} obtained from the g03w anharmonic calculation is practically the same as the anharmonic frequency obtained from the Somorjai−Hornig perturbation treatment described above using the one-dimensional potential from the single point (SCAN) calculation discussed above. The other serious drawback of the g03w procedure is that it does not compute the intensities of the bands in the anharmonic spectrum.

These shortcomings of the g03w anharmonic calculations are important for systems with strong hydrogen bonds as in PANO where the anharmonic frequency of the OH stretch is very low, resulting in strong mixing of the OH stretch with other vibrations. This mixing affects the intensity distribution within the spectrum (see later discussion). Examination of the calculated harmonic and experimental intensities in Table 3 suggests that the large intensity calculated for the OH-stretching mode (574 km/mol) was transferred almost entirely into the bands at 1737 and 1514 cm^{-1} in the experimental spectrum. This crude observation is confirmed by more precise analysis of the anharmonic spectrum based on the relaxed potential discussed in the following sections.

Examination of Table 3 suggests that the procedure in g03w anharmonic does give quite good results for normal vibrations other than the OH stretching mode which are expected to have small anharmonicity.

Anharmonic Spectrum Based on the Relaxed Potential for PANO in the Dielectric Field with $\epsilon = 1.6$. Within this approach, a normal coordinate calculation for PANO in a field with $\epsilon = 1.6$ is carried out, under the assumption that the large anharmonic effect occurs because of the change in shape of the potential energy curve in the cross section along the OH

TABLE 3: Calculated Harmonic Frequencies (ν_{ha}), Intensities (A_{ha}) and Description of Normal Modes (Q*i*) Together with Anharmonic Frequencies from Gaussian 03 (ν_{anhG03}) for PANO in Vacuo Compared with Experimental Frequencies (ν_{exp}) and Integrated Intensities (A_{exp}) of PANO Isolated in an Ar Matrix

Q*i*	ν_{ha} (cm^{-1})	A_{ha} (km/mol)	description of normal modes in terms of internal coordinates[a]	ν_{anhG03} (cm^{-1})	ν_{anh}/ν_{ha} (cm^{-1})	ν_{exp} (cm^{-1})	A_{exp}[b] (km/mol)
			In-Plane Modes				
1	3266	2	12 C6H s	3139	0.961		
2	3241	4	15 C3H s, 14 C4H s	3101	0.957		
3	3230	1	14 C4H s, 13 C5H s, 15 C3H s	3112	0.964		
4	3216	1	13 C5H s, 14 C4H s	3078	0.957		
5	2991	574	1 O2H s	2421	0.809		
6	1841	307	11 C7═O3 s	1801	0.978	1737[c]	720[d]
7	1670	31	5 C5C5 s, 2 C2C3 s, 3 C3C4 s	1629	0.975	1611	10
8	1603	15	4 C4C5 s, 3 C3C4 s, 27 HO2C7 be	1563	0.975	1561	3
9	1564	364	27 HO2C7 be, 26 O3C7 be, 9 C7−O2 s	1513	0.967	1514[c]	525[d]
10	1520	12	20 C4H be, 2 C2C3 s, 5 C5C6 s, 19 C3H be	1488	0.979	1483	69
11	1478	172	21 C5H be, 22 C6H be, 7 NO1 s, 24 C2C7 be	1446	0.978	1439[c]	228[d]
12	1354	132	7 NO1 s, 9 C7−O2 s, 21 C5H be	1321	0.976	1311[c]	120[d]
13	1298	8	2 C2C3 s, 19 C3H be, 10 NC2 s	1268	0.977	1261	32
14	1272	1	6 NC6 s, 19 C3H be, 5 C5C6 s, 10 NC2 s	1245	0.979	1220	2
15	1228	37	9 C7−O2 s, 7 NO1 s, 6 NC6 s	1184	0.964	1165	55
16	1178	2	20 C4H be, 21 C5H be	1162	0.978	1158	1
17	1169	29	9 C7−O2 s, 22 C6H be, 21 C5H be, 3 C3C4 s	1147	0.981	1144	70
18	1112	2	16 Ri de1, 6 NC6 s, 19 C3H be	1090	0.98	1090	7
19	1070	11	4 C4C5 s, 19 C3H be, 3 C3C4 s, 22 C6H be	1046	0.977	1038[c]	26[d]
20	873	21	16 Ri de1, 7 NO1 s, 6 NC6 s, 25 C2C7O2 be	858	0.983	853	24
21	779	6	26 O3C7 be, 8 C7C2 s, 10 NC2 s	766	0.983	762	9
22	664	2	17 Ri de2, 26 O3C7 be, 18 Ri de3	653	0.983	648	2
23	587	24	23 NO1 be, 25 C2C7O2 be, 24 C2C7 be	582	0.991	577[c]	47[d]
24	576	6	18 Ri de3, 17 Ri de2	570	0.99	566	8
25	452	1	25 C2C7O2 be, 23 NO1 be, 24 C2C7 be	449	0.993	*e*	
26	396	13	8 C7C2 s, 18 Ri de3, 26 O3C7 be	393	0.992	*e*	
27	279	23	24 C2C7 be, 25 C2C7O2 be	277	0.993	*e*	
			Out-of-Plane Modes				
28	1005	1	32 oC3H w, 33 oC4H w, 34 oC5H w	988	0.983	976	2
29	975	2	34 oC5H w, 35 oC6H w, 32 oC3H w	957	0.981	972	9
30	925	82	39 oHOC7 t	912	0.986	965	83
31	887	2	35 oC6H w, 33 oC4H w, 32 oC3H w	874	0.985	877	1
32	790	38	33 oC4H w, 34 oC5H w, 36 oC6H w	777	0.983	769	38
33	758	18	28 oRi de1, 37 oOCO tw, 38 oOCO w, 31 oNO1w	762	1.005	768	19
34	678	21	28 oRi de1, 37 oOCO tw, 38 oOCO w, 31 oNO1w	669	0.987	674	23
35	535	3	31 oNO1 w, 30 oRi de3, 28 oRi de1	528	0.987	*e*	
36	442	0	29 oRi de2, 30 oRi de3	435	0.984	*e*	
37	252	4	29 oRi de2, 30 oRi de3, 36 oCC2 w, 31 oNO1w	249	0.988	*e*	
38	130	0	36 oCC2 w, 30 oRi de3	128	0.985	*e*	
39	91	3	38 oOCO w, 37 oOCO tw	91	1	*e*	

[a] Definition of the symmetry coordinates given in Table 1. [b] Normalized experimental integrated intensity (see text). [c] Frequency of the most intense band of the group of bands (see Table 2). [d] Intensity of all components of the group of bands (see Table 2). [e] Below studied region.

stretching coordinate only, and that deviations of the potential energy curves from harmonic, along all other symmetry displacement coordinates, are very small. This assumption is supported by the results presented in the previous section. As shown in Table 3, the values of the ratio of the anharmonic to the harmonic frequency are on the order of 1.0−0.96 for all normal modes except for the OH stretch, for which it is 0.809. It is clear from the comparison with experimental spectrum in previous discussion that the anharmonicity of the OH stretch mode is underestimated in the g03w anharmonic calculation.

In the discussion above the terms "OH-stretching frequency" and "anharmonic potential for the OH stretching vibration" refer to a one-dimensional (1-D) oscillator described by the single mass-weighted displacement coordinate q, where

$$q(\mathrm{OH}) = \mu^{1/2}\,\delta\mathrm{r} = \mu^{1/2}\,\delta r_{\mathrm{O2H}} = \mu^{1/2}\,[R(\mathrm{O2H}) - R_e(\mathrm{O2H})] \quad (1)$$

For PANO in a field with $\epsilon = 1.6$, the 1-D relaxed potential energy associated with stretching the O2H bond was fitted by a fourth order polynomial function of δr:

$$V_{\mathrm{anh}}(\delta r) = a\delta r^4 + b\delta r^3 + c\delta r^2 + d\delta r \quad (2)$$

This function replaced the harmonic potential

$$V_{\mathrm{ha}}(\delta r) = {}^1/_2 k_{\mathrm{ha}} \delta r^2 \quad (3)$$

in the Hamiltonian operator for the 1-D anharmonic oscillator problem, which was solved by the Somorjai−Hornig perturbation treatment[36] to obtain the frequency ν_{anh} of the fundamental ($v = 0 \rightarrow 1$) transition. Another way to state this is to say that the properties of an anharmonic 1-D oscillator in the ground state are modeled, in theory, by replacing the classical harmonic oscillator (with ν_{ha}) by an *effective* harmonic oscillator with an effective frequency ν_{eff} equal to the value of ν_{anh}. For this effective oscillator the potential energy function valid up to the $v = 1$ level is

$$V_{\mathrm{eff}}(\delta r) = {}^1/_2 k_{\mathrm{eff}}\, \delta r^2 \quad (4)$$

From this

$$k_{\mathrm{eff}}/k_{\mathrm{ha}} = [\nu_{\mathrm{eff}}/\nu_{\mathrm{ha}}]^2 \equiv [\nu_{\mathrm{anh}}(\mathrm{OH})/\nu_{\mathrm{ha}}(\mathrm{OH})]^2 \equiv {c_1}^2 \quad (5)$$

assuming that the effective mass for the OH oscillator does not depend on whether it is harmonic, but is always given by $1/\mu = 1/m_{\mathrm{H}} + 1/m_{\mathrm{O}}$. Hence, the effective force constant is

$$k_{\mathrm{eff}} = c_1^{\,2} k_{\mathrm{ha}} \tag{6}$$

A polyatomic molecule such as PANO has $3n - 6$ such 1-D oscillators, each associated with a normal vibration frequency (normal mode) ν_i and a normal coordinate Q*i*, which is a function of the complete set of the independent (nonredundant) symmetry displacement coordinates, S_i, and not just of $S_1 = \delta r_{\mathrm{OH}}$. The harmonic potential energy in the symmetry displacement coordinates has the form:

$$V_{\mathrm{ha}}(S_1, S_2 \cdots S_{3n-6}) = {}^1/_2 k_{11} S_1^{\,2} + \sum_i k_{1i} S_1 S_i + \sum_j \sum_m {}^1/_2 k_{jm} S_j S_m \tag{7}$$

(S_i, S_j and S_m are remaining symmetry coordinates; $i, j, m = 2, 3, \ldots, 3n - 6$, $k_{1i} = k_{i1}$, and $k_{jm} = k_{mj}$). For the harmonic problem we define $S_1 = \delta r_{\mathrm{OH}}$, and k_{11}, k_{1i}, and k_{jm} are the values for the harmonic diagonal and off-diagonal force constants expressed in the symmetry coordinates defined in Table 1. They were obtained by the usual[31] transformation from the values of harmonic force constants in Cartesian coordinates (from g98w) to those in symmetry coordinates, using xtrapack.[30]

For the multidimensional anharmonic problem, discussion in the previous section suggests that anharmonicity of the potential energy along the OH stretch is much greater than along any of the other symmetry coordinates. It is expected that a good first approximation to the multidimensional anharmonic potential energy may be achieved by assuming that its dependence on all symmetry coordinates *except* S_1 is harmonic. The reasoning given above for the 1-D oscillator suggests that the properties of the multidimensional anharmonic oscillator in the ground state may be modeled by replacing the classical oscillator S_1 by the effective harmonic oscillator, S_{eff}. Thus, the $k_{11}S_1^{\,2}$ term in the potential energy expression in eq 7 is replaced by the equivalent effective term

$$k_{\mathrm{eff}} S_1^{\,2} = c_1^{\,2} k_{\mathrm{ha}} S_1^{\,2} \equiv k_{\mathrm{ha}} S_{\mathrm{eff}}^{\,2} \tag{8}$$

where

$$S_{\mathrm{eff}} = c_1 S_1 \tag{9}$$

In fact, S_{eff} replaces S_1 in every term in the harmonic potential energy expression (eq 7) to obtain the effective multidimensional potential W_{anh} of a system with a large anharmonicity for the OH-stretching vibration:

$$W_{\mathrm{anh}}(c_1 S_1, S_2, S_3 \cdots S_{3n-6}) = {}^1/_2 k_{11} c_1^{\,2} S_1^{\,2} + \sum_i k_{1i} c_1 S_1 S_i + \sum_j \sum_m {}^1/_2 k_{jm} S_j S_m \tag{10}$$

The arguments leading to eq 10 indicate that the normal coordinate calculation of the harmonic spectrum may be adjusted for systems, such as PANO (with large anharmonic OH-stretching) to obtain approximate normal coordinates and normal modes for the anharmonic molecule by the following steps. (1) The diagonal force constant of the harmonic OH stretching coordinate (k_{11}), should be replaced the by the corresponding effective diagonal force constant ($k_{11}c_1^{\,2}$). (2) The harmonic off-diagonal elements involving the OH stretching coordinate (k_{1i}, with $i = 2, 3, \ldots, 3n - 6$) should be replaced by the corresponding effective off-diagonal anharmonic force constants ($k_{1i}c_1$). (3) The remaining terms in the force constant matrix for the anharmonic oscillator (involving the double sum shown as the last term in eq 10) are assumed to have the same values as those from the harmonic calculation. (4) Finally the anharmonic spectrum "REL" is obtained using a normal coordinate program (xtrapack,[30] in this case) and data from the output file from the g98w harmonic calculation for PANO in a field with $\epsilon = 1.6$, with modified force constants as described above in steps 1 and 2.

The summary of the procedure just derived in the preceding part for adjusting off-diagonal force constants is consistent with that used by Pulay and co-workers (see, for example, ref 40) to adjust values of the calculated off-diagonal elements of the harmonic force constants matrix. The arguments presented above (eqs 1−10) show that it is reasonable to apply this procedure to the normal coordinate problem of the anharmonic OH stretch.

Table 4 shows the lower left triangle of the symmetric force constant matrix in symmetry coordinates after transformation of the harmonic force constants in Cartesian coordinates (from the g98w computation) for PANO in a field with $\epsilon = 1.6$ that was used in this normal coordinate calculation. The upper part contains the in plane, and the lower part the out-of-plane force constants. To complete the process summarized above the elements of the in-plane part of the matrix in bold face type should be altered by multiplying the diagonal (10, 10) element (in row 10 and column 10) corresponding to the OH stretching coordinate "S_1" by "$c_1^{\,2}$". All other elements in row 10 and in column 10 should be multiplied by "c_1".

We have calculated the anharmonic spectrum "REL" as described above for PANO in a dielectric field with $e = 1.6$ using a range values of ν_{anh} (within the limits of its uncertainty). The spectrum calculated using $\nu_{\mathrm{anh}} = 1700\ \mathrm{cm}^{-1}$ (so that $c_1 = 0.5946$ and $c_1^{\,2} = 0.3536$) resembles most closely the experimental spectrum of PANO isolated in Ar matrix. This simulated spectrum is shown on the bottom of Figure 9. As seen there, the agreement with the experimental spectrum (shown as the top trace in Figure 9) is quite good, although some discrepancies are still apparent.

The reason for some of these discrepancies is that the factors causing the splitting of the experimental bands into several components (e.g., Fermi resonance, as near 1700 cm^{-1}, seen clearly in Figure 4) are not included in the calculated spectrum in Figure 9. It should also be noted that the bands in the calculated spectrum in Figure 9 were drawn with the same widths at half-maximum intensity, while the width of each band in the experimental spectrum is slightly different. Most of these discrepancies are diminished when integrated intensities of bands and all their components are taken into account, as it seen in the following tables.

We believe that the agreement between experimental and calculated anharmonic spectrum shown in Figure 9 (and in the tables below) establishes that the value of the frequency of the anharmonic 1-D OH oscillator that is consistent with the experimental infrared spectrum of PANO isolated in Ar matrix is $\nu_{\mathrm{anh}} = 1700 \pm 15\ \mathrm{cm}^{-1}$.

Analysis of the Anharmonic Spectrum "REL" Based on the Relaxed Potential, and Interpretation of the Experimental Spectrum of PANO Isolated in Argon Matrix

In-Plane Modes. Table 5 collects data in the 1900−1400 cm^{-1} region for the in-plane modes from the calculation of the anharmonic spectrum "REL" (based on the relaxed potential) described above and shown in Figure 9. For each normal mode the values of the frequency (ν), infrared intensity (A), potential energy distributions (PEDs) and intensity distributions (IDs) are given in terms of symmetry coordinates (defined in Table 1). The frequencies and intensities in the experimental spectrum

TABLE 4: Elements (in aJ/Å^2) of the Force Constant Matrix in Symmetry Coordinates for PANO in a Dielectric Field (e = 1.6); Diagonal and Off-Diagonal Elements Related to the OH Stretch are Marked by Bold Numbers

In-Plane Modes

	1	2	3	4	5	6	7	8	9	10	11	12	13	14
1	7.2776													
2	0.8291	7.0818												
3	−0.53	0.7441	7.3252											
4	0.0756	−0.51	0.7596	7.1143										
5	−0.579	0.3111	−0.435	0.843	7.5151									
6	0.7626	−0.392	0.3385	−0.477	0.7627	6.8417								
7	1.0374	0.0975	−0.182	−0.149	−0.039	0.9443	7.0859							
8	1.0109	0.5334	−0.123	−0.24	−0.228	0.0053	0.0155	4.779						
9	−0.575	−0.117	0.0987	0.1253	0.0638	−0.084	0.2305	0.3743	7.7629					
10	**0.3774**	**0.1112**	**−0.068**	**−0.102**	**−0.077**	**0.1576**	**−0.592**	**0.2534**	**0.6874**	**4.62473**				
11	0.1777	−0.012	0.0196	−0.083	−0.045	0.0315	−0.068	0.9924	1.1755	**−0.2272**	13.142			
12	−0.023	−0.014	−0.009	−0.007	0.0698	0.0827	−0.018	−0.001	0.0073	**−0.00972**	0.0016	5.8353		
13	−0.016	−0.018	−0.004	0.0909	0.0735	−0.019	0.0089	0.0005	0.0002	**0.00396**	−3E−04	0.0054	5.6965	
14	−0.016	−0.009	0.0899	0.0864	−0.01	−0.014	−0.007	1E−05	0.0042	**−0.00354**	0.0039	0.0001	0.0046	5.7055
15	−0.012	0.093	0.0765	−0.004	−0.018	−0.014	−0.002	−0.06	0.0016	**0.00247**	0.0083	0.0012	−5E−04	0.0035
16	−0.064	−0.044	−0.003	0.0353	0.0329	0.0656	0.2305	−0.292	−0.038	**−0.0343**	−0.077	−0.088	0.0934	−0.091
17	0.1427	0.2414	0.0701	−0.425	−0.011	0.186	0.2966	0.3772	−0.177	**0.18138**	0.0941	−0.081	0.0354	0.0437
18	0.1128	−0.115	0.2613	−0.054	−0.276	0.1435	−0.37	0.3609	0.0523	**0.02597**	0.0817	0.0146	0.0795	−0.074
19	−7E−04	0.1557	−0.147	−0.008	0.0243	−0.024	0.0126	−0.017	−0.031	**0.01562**	0.041	−3E−04	−0.006	0.0083
20	−0.019	0.0131	0.17	−0.171	−0.013	0.0187	−4E−04	0.0037	0.0057	**−0.00488**	0.0038	−0.005	0.0082	−0.002
21	−0.025	0.0217	−0.015	−0.15	0.1633	0.0147	0.0054	−0.005	−0.002	**0.00522**	0.0039	−0.004	0.0111	0.0075
22	−0.01	−0.028	0.0068	−0.006	−0.129	0.2649	−0.032	0.0069	0.0043	**−0.01112**	0.0076	0.0401	0.0059	−0.006
23	−1.136	−0.048	0.011	0.3231	0.068	0.2898	0.0036	−0.529	0.4765	**−0.1832**	−0.118	−0.045	0.0085	−4E−04
24	−1.425	0.0568	0.1494	0.3399	0.2306	−0.057	−0.169	−0.754	0.4899	**−0.57892**	−0.268	−0.009	0.0058	0.0039
25	0.7203	0.1728	−0.081	−0.307	−0.16	0.0108	0.1462	0.8833	0.3909	**0.79036**	−0.401	0.0013	−0.006	0.0071
26	0.0862	−0.026	−0.041	−0.036	0.0297	0.0254	−0.142	−0.478	0.7021	**−0.20329**	−0.009	−0.005	−0.002	−0.002
27	−0.288	−0.011	0.0365	0.0293	−0.004	−0.053	−0.054	0.1781	0.763	**0.5994**	0.0984	0.0033	−9E−04	−7E−04

	15	16	17	18	19	20	21	22	23	24	25	26	27
15	5.7503												
16	0.0942	1.4133											
17	−0.089	−0.019	1.5158										
18	−0.006	−0.141	0.0643	1.4739									
19	0.0535	0.014	−0.012	−0.093	0.5124								
20	−0.008	0.0007	0.0699	0.0404	0.0092	0.5317							
21	−0.005	0.0008	0.0738	−0.045	0.0107	−0.009	0.5286						
22	6E−05	−0.031	−0.037	0.0854	0.0007	0.0109	0.0056	0.5375					
23	−0.006	0.1059	−0.252	−0.094	−0.011	−0.007	0.0152	−0.023	1.9282				
24	−0.045	0.192	−0.435	−0.252	0.0078	0.0086	−0.001	−0.02	0.991	2.39203			
25	0.0548	−0.217	0.4492	0.2105	−0.008	0.0122	−8E−04	−3E−04	−0.671	−1.33451	3.7954		
26	0.0551	0.051	0.0707	−0.11	−0.001	0.0007	0.0028	−0.008	−0.131	−0.29759	1.3985	2.5102	
27	−4E−04	−0.078	−0.048	0.1072	−0.006	−4E−04	0.0002	0.0021	0.2535	−0.03784	0.6292	0.1899	1.4505

Out-of-Plane Modes

	28	29	30	31	32	33	34	35	36	37	38	39
28	0.3338											
29	−0.01	0.3202										
30	−0.043	0.0054	0.3077									
31	0.1896	−0.089	0.1886	0.8513								
32	0.1385	0.1694	−0.024	−0.002	0.5181							
33	−0.157	−0.08	0.1308	−0.025	−0.075	0.4644						
34	0.1518	−0.098	−0.148	−0.005	−0.005	−0.066	0.4842					
35	−0.15	0.1579	0.0074	−0.089	−0.012	0.0012	−0.071	0.4341				
36	0.0037	−4E−04	0.0278	−0.035	−0.06	0.0018	−0.009	0.0038	0.1632			
37	0.0331	−0.009	0.0493	0.0891	−0.008	0.0011	0.0033	−0.003	−0.019	0.28119		
38	0.0193	−0.004	0.0427	0.0841	−0.008	0.0022	−9E−04	0.0033	−0.002	−0.15386	0.2715	
39	0.054	0.0011	0.0817	0.1591	0.0012	0.0003	0.0015	0.0025	−0.015	0.06804	0.1231	0.2366

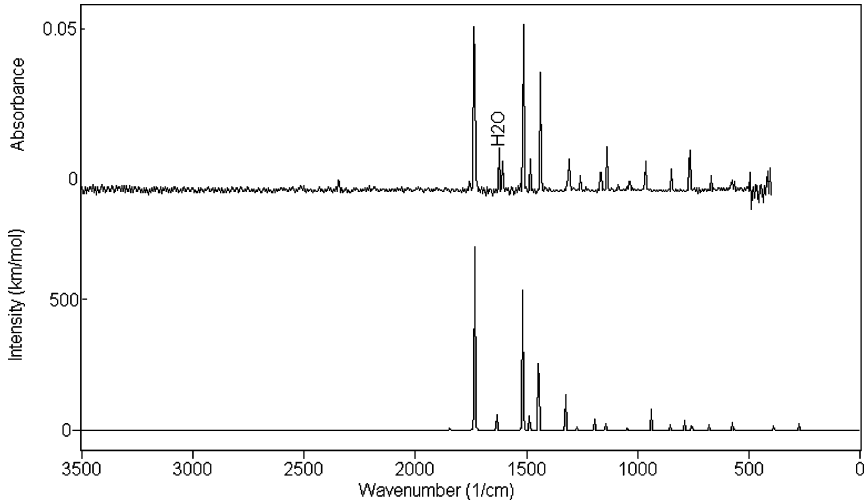

Figure 9. Comparison of the experimental spectrum of PANO isolated in Ar matrix (top trace) with the anharmonic spectrum "REL" of PANO in the field with $\epsilon = 1.6$ (bottom trace). In the calculated spectrum frequencies of all in-plane modes are scaled by a constant factor of 0.98 and the frequencies of all out-of-plane modes are not scaled.

of PANO in the Ar matrix assigned to calculated normal modes in the anharmonic spectrum are listed in bold face type below anharmonic values for a comparison. The criterion for the match is that both frequency and intensity from the calculation should be close to the values from the experimental spectrum. It can be expected that with such a close match the calculated description of the normal modes in terms of internal coordinates as well as the PEDs and the IDs would generally apply to the experimental spectrum providing its interpretation.

Because the results have been presented here as a perturbation of the harmonic spectrum, the corresponding results for the harmonic calculation of the spectrum of PANO in a dielectric field ($\epsilon = 1.6$) are also listed in Table 5. In addition to the unscaled calculated frequencies (in both harmonic and anharmonic spectra) the frequencies scaled by a constant factor 0.98 are also given in Table 5. The scaling factor 0.98 is close to the average ratio of the anharmonic and harmonic frequencies (except for the OH and CH stretch) from the g03w anharmonic given in Table 3. This scaling factor accounts approximately for the basis set error and the anharmonicity of the vibrations other than OH stretch. The CH stretch normal modes are not listed because their frequencies are the same as those given in Table 3. As seen in this table, the calculated values of their intensities are all very low, consistent with the fact that we do not observe any absorption in this region in the spectrum of PANO isolated in the Ar matrix.

The most important observations from examining Table 5 related to the agreement between the corresponding experimental and calculated frequencies and intensities and to the mixing of the OH stretching mode with the other modes in the anharmonic spectrum are discussed below.

1. In sharp contrast to the harmonic spectrum for which the normal mode Q5 at 2859 cm^{-1} (calculated to be very intense) is essentially pure OH stretch (PED = 97%), in the anharmonic spectrum the normal mode Q5 is calculated at 1845 cm^{-1} with very low intensity, and it is a mixture of the C═O stretch (PED = 45%), the OH stretch (PED = 27%) and the in-plane HOC bend (PED = 22%). This mixing of the OH stretch with the in-plane HOC (or HO2C7) bend (in phase) and with the C═O stretch (out of phase) results in a very low intensity (see values of IDs). The normal mode Q5 in the anharmonic spectrum has frequency and intensity close to those found in the experimental spectrum, although the experimental band assigned to this mode

TABLE 5: Comparison of in-Plane Nornal Modes (Q*i*) of the Calculated Anharmonic Spectrum "REL" and the Harmonic Spectrum of PANO in Dielectric Field ($e = 1.6$) with the Experimental Ar Matrix Spectrum (Bold Numbers) in the Spectral Region 1900−1400 cm^{-1}

	calculated anharmonic spectrum "REL"						calculated harmonic spectrum					
	ν_{cal} (cm^{-1}) / ν_{exp} (cm^{-1})		A_{cal} (km/mol) / A_{exp}[c]				ν_{cal} (cm^{-1})		A_{cal}			
Q*i*	Usc[a]	Sc[b]		symmetry coordinate[d]	(PED)[e] (%)	[ID][f] (km/mol)	Usc[a]	Sc[b]	(km/mol)	symmetry coordinate[d]	(PED)[e] (%)	[ID][f] (km/mol)
5	1883	1845	11	11 C7═O3 s	(45+)	[14]	2917	2859	681	1 O2H s	(97+)	[735]
		1867	**10**	1 O2H s	(27−)	[9]						
				27 HO2C7 be	(22−)	[−24]						
				24 C2C7 be	(2+)	[−10]						
				25 C2C7O2 be	(−3−)	[20]						
6	1768	1733	714	1 O2H s	(46+)	[450]	1837	1800	359	11 C7═O3	(76+)	[248]
		1737[g]	**720**[h]	11 C7═O3	(33+)	[225]				25 C2C7O2 be	(3+)	[−139]
				25 C2C7O2 be	(9+)	[−147]				26 O3C7 be	(1−)	[46]
				24 C2C7 be	(−2−)	[111]				24 C2C7 be	(0+)	[103]
7	1667	1634	61	5 C5C6 s	(23−)	[10]	1669	1636	37	5 C5C6 s	(24−)	[10]
		1611[i]	**10**[i]	2 C2C3 s	(20−)	[−2]				2 C2C3 s	(21−)	[1]
				3 C3C4 s	(14+)	[−2]				3 C3C4 s	(13+)	[−3]
				11 C7═O3 s	(4−)	[20]				8 C7C2 s	(1+)	[13]
				1 O2H s	(1−)	[22]				24 C2C7 be	(1+)	[−21]
8	1603	1571	4	4 C4C5 s	(31−)	[−3]	1605	1573	37	4 C4C5 s	(28−)	[−3]
		1561	**3**	3 C3C4 s	(17+)	[2]				3 C3C4 s	(15+)	[5]
				10 NC2 s	(9−)	[5]				27 HO2C7 be	(9−)	[30]
9	1549	1518	563	27 HO2C7 be	(59−)	[306]	1577	1545	389	27 HO2C7 be	(75−)	[301]
		1514[g]	**525**[h]	1 O2H s	(14+)	[236]				26 O3C7 be	(3−)	[63]
				26 O3C7 be	(5−)	[110]				9 C7−O2 s	(2+)	[49]
				8 C7C2 s	(4−)	[67]						
10	1518	1488	65	20 C4H be	(20−)	[9]	1520	1490	8	20 C4H be	(20−)	[2]
		1483	**69**	5 C5C6 s	(18−)	[11]				2 C2C3 s	(19+)	[−2]
				2 C2C3 s	(17+)	[−3]				5 C5C6 s	(19−)	[4]
				23 NO1be	(7+)	[−30]				19 C3H be	(13−)	[6]
				27 HO2C7 be	(5+)	[30]						
				1 O2H s	(2−)	[32]						
				24 C2C7 be	(0+)	[24]						
11	1475	1446	277	21 C5H be	(21+)	[18]	1477	1447	193	21 C5H be	(22+)	[18]
		1439[g]	**228**[h]	22 C6H be	(20+)	[17]				22 C6H be	(20+)	[12]
				3 C3C4 s	(11+)	[10]				9 C7−O2 s	(2+)	[19]
				10 NC2 s	(7−)	[29]				10 NC2 s	(7−)	[21]
				7 NO1 s	(5+)	[82]				7 NO1 s	(6+)	[80]
				24 C2C7 be	(4−)	[−112]				19 C3H be	(5+)	[19]
				26 O3C7 be	(2−)	[45]				24 C2C7 be	(4−)	[−83]
				1 O2H s	(1+)	[35]				26 O3C7 be	(1−)	[26]
				27 HO2C7 be	(1−)	[43]				25 C2C7O2 be	(1−)	[24]
				8 C7C2 s	(1−)	[21]						

[a] Usc = unscaled frequencies. [b] Sc = frequencies scaled by 0.98. [c] Normalized experimental integrated intensity (see text). [d] Definition of the symmetry coordinates given in Table 1. [e] See ref 32; the sign at the right side of the PED value indicates its phase relative to the first value listed for the normal mode. [f] See ref 33; for ID the sign indicates whether the contribution adds (+) or subtracts (−) to increase or decrease of total intensity. [g] Frequency of the most intense band of the group of bands (see Table 2). [h] Intensity of the all components of the group of bands (see Table 2). [i] Band can be hidden under the absorption in this region by the H_2O impurities.

is barely distinguishable from the noise and its frequency and intensity are uncertain.

2. The normal mode Q6 (at 1733 cm^{-1}) in the calculated anharmonic spectrum "REL" has frequency and intensity very close to those found for the corresponding mode in the experimental spectrum. This very intense normal mode has its largest contribution to the PED (45%) and ID (450 km/mol) from the OH stretch and a smaller but significant contribution from the C═O stretch (PED = 33%, ID = 225 km/mol). This is in sharp contrast to the harmonic spectrum for which normal mode Q6 (at 1800 cm^{-1}) is dominated by the C═O stretch (PED = 76% and ID = 248 km/mol).

3. The other normal mode of anharmonic spectrum "REL" calculated with very high intensity is Q9 (at 1518 cm^{-1}). Its frequency and intensity are very close to the corresponding experimental values. This normal mode has its largest contribution from the in-plane HOC bending coordinate (PED = 59%, ID = 306 km/mol), but also has a substantial contribution, particularly to the intensity, from the OH-stretching coordinate (PED = 14%, ID = 236 km/mol).

4. The calculated anharmonic spectrum "REL" in Table 5 lists two CH-bending normal modes, Q10 and Q11, at 1488 and 1446 cm^{-1}, with relatively small contributions to PEDs but with significant IDs, from both the OH stretch and HOC bend. Frequencies and intensities of these modes in anharmonic spectrum "REL" are close to those in the experimental spectrum.

The quality of the agreement between the experimental and calculated anharmonic spectrum "REL" for the remaining normal modes is quite good as can be seen by examining Tables 6 (1400−800 cm^{-1}) and 7 (800−270 cm^{-1}). Most of the calculated frequencies agree with the experimental values within ±3%. With a few exceptions, the agreement between calculated and experimental intensities is within ±20% (within the error

TABLE 6: Comparison of in-Plane Nornal Modes (Q*i*) of the Calculated Anharmonic Spectrum "REL" and the Harmonic Spectrum of PANO in Dielectric Field (e = 1.6) with the Experimental Ar Matrix Spectrum (Bold Numbers) in the Spectral Region 1400−800 cm^{-1}

	calculated anharmonic spectrum "REL"						calculated harmonic spectrum					
	ν_{cal} (cm^{-1}) / ν_{exp} (cm^{-1})		A_{cal} (km/mol) / A_{exp}[c]				ν_{cal} (cm^{-1})		A_{cal}			
Q*i*	Usc[a]	Sc[b]		symmetry coordinate[d]	(PED)[e] (%)	[ID][f] (km/mol)	Usc[a]	Sc[b]	(km/mol)	symmetry coordinate[d]	(PED)[e] (%)	[ID][f] (km/mol)
12	1352	1325	147	7 NO1 s	(22+)	[93]	1352	1325	155	7 NO1 s	(22+)	[94]
		1311[g]	**120**[h]	9 C7−O2 s	(16+)	[36]				9 C7−O2 s	(17+)	[37]
				21 C5H be	(12−)	[−9]				21 C5H be	(12−)	[−9]
				22 C6H be	(10−)	[−8]				22 C6H be	(10−)	[−9]
				16 Ri def1	(8−)	[−16]				16 Ri def1	(8−)	[−16]
				8 C7C2 s	(7−)	[33]				8 C7C2 s	(7−)	[35]
				26 O3C7 be	(3−)	[46]				26 O3C7 be	(3−)	[49]
				24 C2C7 be	(0−)	[−41]				24 C2C7 be	(0−)	[−43]
13	1298	1272	13	2 C2C3 s	(27−)	[−3]	1298	1272	12	2 C2C3 s	(27+)	[−3]
		1261	**32**	10 NC2 s	(16+)	[−9]				10 NC2 s	(16−)	[−8]
				19 C3H be	(15−)	[−6]				19 C3H be	(15+)	[−6]
				25 C2C7O2 be	(4+)	[−19]				25 C2C7O2 be	(4−)	[−18]
				7 NO1 s	(4+)	[11]				24 C2C7 be	(2−)	[20]
				9 C7−O2 s	(4+)	[5]						
				24 C2C7 be	(2+)	[22]						
				8 C7C2 s	(1−)	[4]						
14	1271	1246	1	6 NC6 s	(27+)	[−1]	1272	1247	1	6 NC6 s	(25−)	[−1]
		1220	**2**	19 C3H be	(16−)	[−1]				19 C3H be	(15+)	[−1]
				22 C6H be	(13+)	[1]				5 C5C6 s	(13+)	[0]
15	1218	1194	47	9 C7−O2 s	(26−)	[−27]	1226	1201	40	9 C7−O2 s	(28−)	[−25]
		1165[g]	**55**[h]	7 NO1 s	(26+)	[64]				7 NO1 s	(27+)	[54]
				8 C7C2 s	(10+)	[−14]				6 NC6 s	(11−)	[6]
				27 HO2C7 be	(5−)	[20]				8 C7C2 s	(11+)	[0]
				1 O2H s	(3+)	[16]				27 HO2C7 be	(5−)	[10]
				26 O3C7 be	(0+)	[−15]						
16	1177	1154	1	20 C4H be	(32−)	[0]	1178	1154	2	20 C4H be	(33−)	[−1]
		1158	**1**	21 C5H be	(27−)	[1]				21 C5H be	(27−)	[1]
				19 C3H be	(10+)	[−1]				19 C3H be	(10+)	[0]
17	1169	1145	33	9 C7−O2 s	(19−)	[18]	1169	1145	33	9 C7−O2 s	(19−)	[18]
		1144[g]	**70**[h]	22 C6H be	(15+)	[−1]				22 C6H be	(14+)	[−1]
				3 C3C4 s	(14+)	[−3]				3 C3C4 s	(14+)	[−3]
				21 C5H be	(12−)	[5]				21 C5H be	(12−)	[5]
				7 NO1 s	(1−)	[7]						
18	1113	1091	2	16 Ri def1	(26−)	[3]	1114	1092	2	16 Ri def1	(26−)	[2]
		1090	**7**	6 NC6 s	(14+)	[2]				6 NC6 s	(14+)	[1]
				19 C3H be	(13+)	[−2]				19 C3H be	(13+)	[−2]
19	1070	1048	11	4 C4C5 s	(44−)	[−2]	1070	1048	11	4 C4C5 s	(44−)	[−2]
		1038[g]	**26**[h]	19 C3H be	(12+)	[5]				19 C3H be	(12+)	[5]
				3 C3C4 s	(12−)	[−1]				3 C3C4 s	(12−)	[−1]
				24 C2C7 be	(1+)	[5]						
20	871	854	24	16 Ri def1	(43+)	[9]	871	854	25	16 Ri def1	(43+)	[9]
		853	**24**	7 NO1 s	(18+)	[22]				7 NO1 s	(18+)	[22]
				6 NC6 s	(11+)	[−3]				6 NC6 s	(11+)	[−3]

[a] Usc − unscaled frequencies. [b] Sc − frequencies scaled by 0.98. [c] Normalized experimental integrated intensity (see text). [d] Definition of the symmetry coordinates given in Table 1. [e] See ref 32; the sign at the right side of the PED value indicates its phase relative to the first value listed for the normal mode. [f] See ref 33; for ID the sign indicates whether the contribution adds (+) or subtracts (−) to increase or decrease of total intensity. [g] Frequency of the most intense band of the group of bands (see Table 2). [h] Intensity of the all components of the group of bands (see Table 2).

TABLE 7: Comparison of in-Plane Normal Modes (Q*i*) of the Calculated Anharmonic Spectrum "REL" and the Harmonic Spectrum of PANO in Dielectric Field ($\epsilon = 1.6$) with the Experimental Ar Matrix Spectrum (Bold Numbers) in the Spectral Region 800−270 cm^{-1}

	calculated anharmonic spectrum "REL"						calculated harmonic spectrum					
	ν_{cal} (cm^{-1}) / ν_{exp} (cm^{-1})		A_{cal} (km/mol) / A_{exp}[c]				ν_{cal} (cm^{-1})		A_{cal}			
Q*i*	Usc[a]	Sc[b]		symmetry coordinate[d]	(PED)[e] (%)	[ID][f] (km/mol)	Usc[a]	Sc[b]	(km/mol)	symmetry coordinate[d]	(PED)[e] (%)	[ID][f] (km/mol)
21	778	762	6	26 O3C7 be	(28−)	[−8]	780	762	6	26 O3C7 be	(30−)	[−1]
		762	**9**	8 C7C2 s	(18−)	[−2]				8 C7C2 s	(17−)	[1]
				10 NC2 s	(16−)	[−1]				10 NC2 s	(15−)	[0]
				7 NO1 s	(4−)	[5]						
				9 C7−O2 s	(7−)	[2]						
22	662	649	1	17 Ri def2	(42+)	[0]	664	651	2	17 Ri def2	(41+)	[3]
		648	**2**	26 O3C7 be	(34+)	[−2]				26 O3C7 be	(33+)	[4]
23	587	576	34	23 NO1be	(59+)	[29]	588	577	29	23 NO1be	(58+)	[27]
		577[g]	**47**[h]	25 C2C7O2 be	(16−)	[21]				25 C2C7O2 be	(17−)	[20]
				24 C2C7 be	(−3+)	[−23]				24 C2C7 be	(−3+)	[−22]
				1 O2H s	(0+)	[5]						
24	576	564	7	18 Ri def3	(39−)	[2]	576	564	8	18 Ri def3	(39−)	[2]
		566	**8**	17 Ri def2	(28+)	[−1]				17 Ri def2	(28+)	[−2]
				26 O3C7 be	(7−)	[4]						
				24 C2C7 be	(6+)	[4]						
				7 NO1 s	5+	[3]						
25	454	445	1	25 C2C7O2 be	(42+)	[−1]	454	445	1	25 C2C7O2 be	(42+)	[−1]
		j		23 NO1be	(25+)	[1]				23 NO1be	(25+)	[1]
				24 C2C7 be	(15+)	[1]				24 C2C7 be	(15+)	[1]
26	398	390	21	8 C7C2 s	(31+)	[6]	399	391	16	8 C7C2 s	(31+)	[5]
		j		18 Ri def3	(19+)	[1]				18 Ri def3	(19+)	[1]
				26 O3C7 be	(14−)	[−11]				26 O3C7 be	(13−)	[−9]
				25 C2C7O2 be	(9+)	[9]						
				1 O2H s	(1−)	[7]						
27	279	274	31	24 C2C7 be	(67−)	[23]	280	275	26	24 C2C7 be	(67−)	[21]
		j		25 C2C7O2 be	(20+)	[10]				25 C2C7O2 be	(20+)	[9]
				1 O2H s	(0−)	[5]						

[a] Usc = unscaled frequencies. [b] Sc = frequencies scaled by 0.98. [c] Normalized experimental integrated intensity (see text). [d] Definition of the symmetry coordinates given in Table 1. [e] See ref 32; the sign at the right side of the PED value indicates its phase relative to the first value listed for the normal mode. [f] See ref 33; for ID the sign indicates whether the contribution adds (+) or subtracts (−) to increase or decrease of total intensity. [g] Frequency of the most intense band of the group of bands (see Table 2). [h] Intensity of the all components of the group of bands (see Table 2). [j] Below the studied region.

of measurement and normalization of experimental intensities and the uncertainty of the calculation).

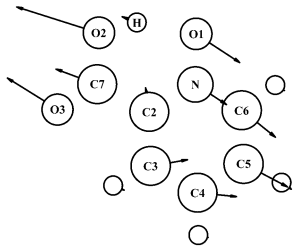

$Q26_{anh}$; $\nu = 390$ cm^{-1}; A = 21 km/mol

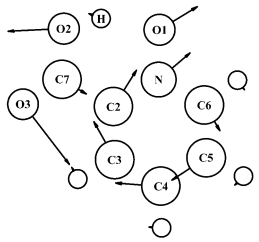

$Q27_{anh}$; $\nu = 274$ cm^{-1}; A = 31 km/mol

Figure 10. Calculated (at DFT/B3LYP/6-31G(d,p) level) atomic displacements (in Cartesian coordinates) in the low-frequency normal modes at 390 and 274 cm^{-1} with the largest contribution from the O1···O2 stretching vibration.

Unfortunately, the very low signal-to-noise ratio of the spectrometer and its low-frequency cutoff (at 400 cm^{-1}) made it impossible to record the experimental spectrum in the region below 550 cm^{-1}. The normal modes involving the "heavy atom" O1···O2 stretch are located in this region. Even though there are no experimental data to test the results of the calculations, this motion is so important in the interpretation of spectra for hydrogen bonded systems using 2-dimensional models that we shall discuss them briefly here.

The "heavy atom" O1···O2 stretch is not an independent degree of freedom for a bent intramolecular OHO system because of the geometric constraints. For this reason the O1···O2 distance change is not used as one of the symmetry coordinates. Because of that, the PEDs given in Table 7 for the normal modes Q26 and Q27 do not reflect the O1···O2 motion. Instead, it is described in terms of stretching and bending symmetry coordinates such as C2C7 bend, C2C7 stretch, and C2C7O2 bend and others.

Involvement of the O1···O2 stretch in these normal modes is recognizable better in Figure 10, which shows by arrows the unweighted Cartesian displacement coordinates for normal modes Q26 (at 390 cm^{-1}) and Q27 (at 274 cm^{-1}). The figure, drawn using the animol program,[29] shows the displacements in Cartesian coordinates (from g98w); hence, they are independent of the definition of symmetry coordinates. As seen in this figure, in addition to the O1···O2 stretching, each mode shows extensive displacements of most of the other atoms in the molecule. Thus, Q26 is primarily a motion in which the entire H−O2−C7═O3 unit moves against the pyridine *N*-oxide unit

resulting in an increase of the O1···O2 distance. In normal mode Q27, the H−O2−C7═O3 unit rotates counterclockwise against the clockwise rotation of the pyridine *N*-oxide unit, again resulting in an increase in the O1···O2 distance. This figure also shows the small contribution from the O2H stretch in Q26 and Q27.

Out-of-Plane Modes. Because the perturbations of the harmonic calculation of the spectrum used in the model calculation of anharmonic spectrum "REL" are all in the plane of the PANO molecule, the calculated spectrum for the out-of-plane motions is identical to the spectrum calculated at harmonic approximation. Table 8 collects calculated frequencies (unscaled, and scaled by a factor of 0.98), intensities and the description of the normal modes in terms of symmetry coordinates at the harmonic approximation of the out-of-plane modes of PANO in the field with $\epsilon = 1.6$. As seen in this table, most of the calculated frequencies agree with the experimental values within ±3%. The agreement between calculated and experimental intensities is also within the uncertainty in the data. The anharmonicity of the out-of-plane modes can be estimated by examination of Table 3.

TABLE 8: Comparison of the out-of-Plane Normal Modes (Q*i*) of the Calculated Harmonic Spectrum of PANO in Dielectric Field ($\epsilon = 1.6$) with Experimental Ar Matrix Spectrum (Bold Numbers)

	calculated anharmonic spectrum "REL"					
	ν_{cal} (cm^{-1}) / ν_{exp} (cm^{-1})		A_{cal} (km/mol) / A_{exp}[c]			
Q*i*	Usc[a]	Sc[b]		symmetry coordinate[d]	(PED)[e] (%)	[ID][f] (km/mol)
28	1007	987	1	32 oC3H w	(54+)	[3]
		976	**2**	33 oC4H w	(50−)	[−3]
				34 oC5H w	(16−)	[1]
29	978	958	2	34 oC5H w	(63+)	[−5]
		972	**9**	32 oC3H w	(26−)	[3]
				35 oC6H w	(25−)	[4]
30	942	923	83	39 oHOC7 t	(101−)	[88]
		965	**83**			
31	890	872	2	35 oC6H w	(60+)	[5]
		877	**1**	33 oC4H w	(20−)	[−2]
				32 oC3H w	(19−)	[−2]
32	792	776	40	33 oC4H w	(33−)	[14]
		769	**38**	34 oC5H w	(26−)	[12]
				35 oC6H w	(18−)	[15]
				31 oNO1 w	(6+)	[14]
				37 oOCO tw	(5−)	[−15]
33	758	742	20	28 oRidef1	(27−)	[−15]
		768	**19**	37 oOCO tw	(23+)	[18]
				38 oOCO w	(22−)	[−7]
				31 oNO1 w	(19+)	[22]
34	679	665	22	28 oRidef1	(57+)	[18]
		674	**23**	37 oOCO tw	(19+)	[16]
				38o OCO w	(12−)	[−4]
				31 oNO1 w	(9−)	[−20]
35	534	523	3	31 oNO1 w	(42−)	[−8]
		g		30 oRidef3	(31+)	[6]
				28 oRidef1	(26−)	[−3]
36	441	432	0	29 oRidef2	(78−)	[0]
		g		30 oRidef3	(23−)	[0]
37	253	248	4	29 oRidef2	(30+)	[1]
		g		30 oRidef3	(30−)	[2]
				36 oCC2 w	(16−)	[0]
				31 oNO1 w	(15−)	[2]
38	132	129	0	36 oCC2 w	(70+)	[0]
		g		30 oRidef3	(26−)	[0]
39	92	90	3	38 oOCO w	(63+)	[2]
		g		37 oOCO tw	(38+)	[4]

[a] Usc − unscaled frequencies. [b] Sc − frequencies scaled by 0.98. [c] Normalized experimental integrated intensity (see text). [d] Definition of the symmetry coordinates given in Table 1. [e] See ref 32; the sign at the right side of the PED value indicates its phase relative to the first value listed for the normal mode. [f] See ref 33; for ID the sign indicates whether the contribution adds (+) or subtracts (−) to increase or decrease of total intensity. [g] Below studied region.

Concluding Remarks

(1) It is obvious that the quantum-mechanical DFT/B3LYP//6-31G(d,p) calculation of the spectrum of PANO at the harmonic approximation does not resemble the experimental spectrum. Not only there is no intense absorption band within 1200 cm^{-1} of the calculated harmonic frequency for the OH stretch near 2900 cm^{-1} but also there is no absorption at all that is clearly distinguishable from the noise. At first glance, it appears as though the strong infrared absorption band expected for the OH stretching mode has simply disappeared, leaving no trace.

(2) The mixing of the OH stretching with other internal coordinates in the calculated anharmonic spectrum "REL" that agrees with the experimental spectrum of PANO isolated in Ar matrix clearly answers the question "What has happened to the strong absorption from the OH stretch?" It is no longer associated with one single strong band but most of the intensity associated with the OH stretch is accounted for in anharmonic spectrum "REL" by intensity redistribution into the normal modes Q6 and Q9, causing significant enhancements of their intensity. Our experience from this and other studies of PANO and other systems with strong hydrogen bonds[41] suggests that the mixing of the OH stretch with other modes does not become significant until the effective frequency for the OH-stretching normal mode drops below about 2200 cm^{-1} and that mixing becomes more important the lower it becomes.

(3) In the analysis of the experimental infrared spectrum of PANO isolated in an Ar matrix, and in its interpretation, it is hard to overemphasize the importance of the infrared intensity. It is true that measuring the absolute integrated molar absorption coefficients of the bands observed in the spectrum may have considerable error (perhaps as large as 20% or even 50% for some less intense or overlapped bands). However, even such uncertain estimates of intensities are extremely valuable in an attempt to understand a spectrum like that of PANO. We have seen in the results presented here that, with the exception of the OH stretch, all other frequencies are not very different going from harmonic to anharmonic spectrum "REL", but the intensity pattern differs dramatically.

(4) The agreement between the anharmonic spectrum "REL" and the experimental infrared spectrum of PANO in an Ar matrix shown in Figure 9 and in Tables 5−8 is surprisingly good, and strongly supports the validity of our approach. The anharmonic spectrum "REL" is perhaps the simplest possible model. Some of the assumptions in it may be questioned. It is possible that alternate models based on different assumptions might be developed to calculate anharmonic spectra (and we have tried many of them[41]). However, the apparent success of anharmonic spectrum "REL" in understanding the experimental spectrum of PANO suggests very strongly that the essential concepts are indeed valid, and that further refinements will not change the interpretation of the spectrum very much.

(5) A general conclusion from the studies presented here is that the relaxed potential energy curve may provide a reasonably good approximation to the "true" potential for the strongly anharmonic stretching motion of the hydrogen atom in other short and strong hydrogen bonds. However, more studies are needed (and are in progress[41]) to justify this generalization.

References and Notes

(1) Stare, J.; Mavri, J.; Ambrožić, G.; Hadži, D. *J. Mol. Struct. (THEOCHEM)* **2000**, *500*, 429.

(2) Laing, M.; Nicholson, C. J. S. *Afr. Chem. Inst.* **1971**, *24*, 186.

(3) Steiner, T.; Schreurs, A. M. M.; Lutz, M.; Kroon, J. *Acta Crystallogr. C* **2000**, *56*, 577.
(4) Szafran, M. *Bull. Acad. Polon. Sci. Chim.* **1965**, *18*, 245.
(5) Dega-Szafran, Z.; Grunwald-Wyspianska, M.; Szafran, M. *J. Mol. Struct.* **1992**, *275*, 159.
(6) Eckert, J.; Hadži, D. Manuscript in preparation 2004.
(7) Tayyaari, S. F.; Zeegers Huyskens, T.; Wood, J. L. *Spectrochim. Acta A* **1979**, *35*, 1265.
(8) Bertolasi, V.; Gilli, P.; Perretti, V.; Gilli, G. *J. Am. Chem. Soc.* **1991**, *113*, 4917.
(9) Emsley, J.; Lyy, M. A.; Bates, P. A.; Hursthouse, M. B. *J. Mol. Struct.* **1988**, *178*, 297.
(10) Stare, J.; Balint-Kurti, G. G. *J. Phys. Chem. A* **2003**, *107*, 7204.
(11) Stare, J.; Mavri, J. *Comput. Phys. Commun.* **2002**, *143*, 222.
(12) Panek, J.; Stare, J.; Hadži, D. *J. Phys. Chem. A* **2004**, *108*, 7417.
(13) Avbelj, F.; Hodošček, M.; Hadži, D. *Spectrochim. Acta A* **1985**, *41*, 89.
(14) Chiavassa, T.; Roubin, P.; Pizzala, L.; Verlaque, P.; Allouche, A.; Marinelli, F. *J. Phys. Chem.* **1992**, *96*, 10659.
(15) Meyer, R.; Ha, T.-K. *Mol. Phys.* **2003**, *101*, 3263.
(16) Alparone, A.; Millefiori, S. *Chem. Phys.* **2003**, *290*, 15.
(17) Došlić, N.; Kühn, O. *Z. Phys. Chem.* **2003**, *217*, 1507.
(18) (a) Hohenberg, P.; Kohn, W. *Phys. Rev. B* **1964**, *136*, 864. (b) Kohn, W.; Sham, L. J. *Phys. Rev. A* **1965**, *140*, 1133. (c) Parr, R. G.; Yang, W. *Density Functional Theory of Atoms and Molecules*; Oxford University Press: New York, 1989. (d) Jones, R. O.; Gunnarsson, O. *Rev. Modern Phys.* **1989**, *61*, 689. (e) Ziegler, T. *Chem. Rev.* **1991**, *91*, 651. (f) Becke, A. D. *Phys. Rev. A* **1988**, *38*, 3098. (g) Becke, A. D. *J. Chem. Phys.* **1992**, *97*, 9173. (h) Becke, A. D. *J. Chem. Phys.* **1993**, *98*, 5648. (i) Lee, C.; Yang, W.; Parr, R. G. *Phys. Rev. B* **1988**, *37*, 785. (j) Vosko, S. H.; Wilk, L.; Nussair, M. *Can. J. Phys.* **1980**, *58*, 1200.
(19) Frisch, M. J.; Trucks, G. W.; Schlegel, H. B.; Scuseria, G. E.; Robb, M. A.; Cheeseman, J. R.; Zakrzewski, V. G.; Montgomery, J. A., Jr.; Stratmann, R. E.; Burant, J. C.; Dapprich, S.; Millam, J. M.; Daniels, A. D.; Kudin, K. N.; Strain, M. C.; Farkas, O.; Tomasi, J.; Barone, V.; Cossi, M.; Cammi, R.; Mennucci, B.; Pomelli, C.; Adamo, C.; Clifford, S.; Ochterski, J. W.; Petersson, G. A.; Ayala, P. Y.; Cui, Q.; Morokuma, K.; Malick, D. K.; Rabuck, A. D.; Raghavachari, K.; Foresman, J. B.; Cioslowski, J.; Ortiz, J. V.; Stefanov, B. B.; Liu, G.; Liashenko, A.; Piskorz, P.; Komaromi, I.; Gomperts, R.; Martin, R. L.; Fox, D. J.; Keith, T.; Al-Laham, M. A.; Peng, C. Y.; Nanayakkara, A.; Gonzalez, C.; Challacombe, M.; Gill, P. M. W.; Johnson, B.; Chen, W; Wong, M. W.; Andres, J. L.; Gonzalez, C.; Head-Gordon, M.; Replogle, E. S.; Pople, J. A. *Gaussian* 98, Revision A.3; Gaussian, Inc.: Pittsburgh, PA, 1998.
(20) Frisch, M. J.; Trucks, G. W.; Schlegel, H. B.; Scuseria, G. E.; Robb, M. A.; Cheeseman, J. R.; Montgomery, J. A., Jr.; Vreven, T.; Kudin, K. N.; Burant, J. C.; Millam, J. M.; Iyenger, S. S.; Tomasi, J.; Barone, V.; Mennucci, B.; Cossi, M.; Scalmani, G.; Rega, N.; Petersson, G. A.; Nakatsuji, H.; Hada, M.; Ehara, M.; Toyota, K.; Fukuda, R.; Hasegawa, J.; Ishida, M.; Nakajima, T.; Honda, Y.; Kitao, O.; Nakai, H.; Klene, M.; Li, X.; Knox, J. E.; Hratchian, H.; Cross, J. B.; Adamo, C.; Jaramillo, J.; Gomperts, R.; Strautmann, E.; Yazyev, O.; Austin, A. J.; Cammi, R.; Pomelli, C.; Ochterski, J. W.; Ayala, P. Y.; Morokuma, K.; Voth, G. A.; Salvador, P.; Dannenberg, J. J.; Zakrzewski, V. G.; Dapprich, S.; Daniels, A. D.; Strain, M. C.; Farkas, O.; Malick, D. K.; Rabuck, A. D.; Raghavachari, K.; Foresman, J. B.; Ortiz, J. V.; Cui, Q.; Baboul, A. G.; Clifford, S.; Cioslowski, J.; Stefanov, B. B.; Liu, G.; Liashenko, A.; Piskorz, P.; Komaromi, I.; Martin, R. L.; Fox, D. J.; Keith, T.; Al-Laham, M. A.; Peng, C. Y.; Nanayakkara, A.; Challacombe, M.; Gill, P. M. W.; Johnson, B.; Chen, W.; Wong, M. W.; Gonzalez, C.; Pople, J. A. *Gaussian 03W* Revision A1; Gaussian, Inc.: Pittsburgh PA, 2003.
(21) Foresman, J. B.; Frisch, A. E. *Exploring Chemistry with Electronic Structure Methods*; Gaussian, Inc.: Pittsburgh, PA, 1996.
(22) (a) Frisch, M. J.; Frisch, M. J. *Gaussian 98, User's Reference*, 2nd ed.; Gaussian, Inc.; Pittsburgh, PA.; 1999. (b) Frish, A. E.; Frisch, M. J.; Truck, G. W. *GAUSSIAN 03, User's Reference*; Gaussian, Inc.: Pittsburgh, PA, 2003.
(23) Person, W. B. In *Matrix Isolation Spectroscopy*; Barnes, A. J., Orville-Thomas, W. J., Muller, A., Gaufres, R., Eds.; NATO ASI Series C, D. Reidel: Dordrecht, The Netherlands, 1981; Vol. 76, pp 415−445.
(24) Szczepaniak, K.; Szczesniak, M. M.; Person, W. B. *J. Phys. Chem. A* **2000**, *104*, 3852.
(25) Person, W. B.; Szczepaniak, K.; Kwiatkowski, J. S. *Int. J. Quantum Chem.* **2002**, *90*, 995.
(26) Person, W. B.; Szczepaniak, K.; Szczesniak, M.; Del Bene, J. E. In *Recent Experimental and Computational Advances in Molecular Spectroscopy*; Fausto, R., Ed.; NATO ASI Series; Kluwer Academic Publishers: Dordrecht, The Netherlands, 1993; Vol. 406, pp 141−169.
(27) *grams/32* V4.0. Galactic Industries Corp.; 1996.
(28) Moscovits, M., Ozin, G. A., Eds. *Cryochemistry*; J. Wiley & Sons: New York; 1976; p 24.
(29) *Animol 3.2*; *Infrared and Raman Spectroscopy Teaching and Research Tool for Windows*; Innovative Software: Gainesville, FL.; 1996.
(30) Chabrier, P.; Person, W. B. *Program XTRAPACK* (see Chabrier, P. Ph. D. dissertation, University of Florida, 1998). The evolution of this program from the University of Minnesota program *CHARLY* was traced in ref 22 given in ref 24.
(31) (a) Wilson, E. B., Jr.; Decius, J. C.; Cross, P. C. *Molecular Vibrations*; McGraw-Hill: New York, 1955. See also: (b) Califano, S. *Vibrational States* Wiley: London; 1976.
(32) (a) Morino, Y.; Kuchitsu, K. *J. Chem. Phys.* **1952**, *20*, 1809. (b) Keresztury, B.; Jalsovszky, G. *J. Mol. Struct.* **1971**, *10*, 304. Excellent discussions of PEDs can be found in ref 31b and in numerous articles by Mills, I. (see for example Hedberg, L.; Mills, I. *J. Mol. Spectrosc.* **1993**, *160*, 117). The PEDs used in this paper (as they were defined by Keresztury and Jalsovszky), are called TEDs by Pulay, P.; Török, F. *Acta Chim. Hung.* **1965**, *44*, 287.
(33) The value of ID_{ks} is defined as the contribution from the "k" symmetry coordinate to the total intensity, A_s, of the "s" normal mode of vibration. In the notation of Califano, (ref 31b), $ID_{ks} = K\{\Sigma_l L_{ks}[\Sigma_\alpha P_R)_\alpha kP_R)_{\alpha l}]L_{ls}\}$. The units conversion factor ($K = 974.9$) converts from dipole derivatives in (e $u^{1/2}$) to the integrated molar absorption coefficient, A_s, in km/mol; L_{ks} is the k, s element of the normal coordinate transformation matrix $\mathbf{L}$ ($\mathbf{R} = \mathbf{L}\ \mathbf{Q}$); $\mathbf{P}_R$ is the polar tensor in internal (or symmetry) coordinates (see Person, W. B.; Newton, J. *J. Chem. Phys.* **1974**, *61*, 1040), and α designates the Cartesian component (x, y, or z). Note that $A_s = \Sigma_k ID_{ks.}$ Similar ideas were presented by: Qian, W.; Krimm, S. *J. Phys. Chem.* **1993**, *97*, 11578, who introduced an approximate definition of ID that omits the sum over l.
(34) Herzberg, G. *Molecular Spectra and Molecular Structure*; Van Nostrand Reinhold Co: New York, 1945; Vol. 2, pp 215−219.
(35) Hallam, H. E., Ed.; *Vibrational Spectroscopy of Trapped Species*; Wiley: London, 1973.
(36) Somorjai, R. I.; Hornig, D. F. *J. Chem. Phys.* **1962**, *36*, 1980.
(37) Szczepaniak, K.; Chabrier, P.; Person, W. B.; Del Bene, J. E. *J. Mol. Struct.* **2000**, *520*, 1.
(38) Steiner, T. Unpublished results quoted in refs 11 and 12.
(39) We have performed a calculation of the frequencies and intensities of the spectrum corresponding to $\nu_{anh}(OHs) = 2421\ cm^{-1}$ using the normal coordinate program XTRAPACK following the procedure used to obtain anharmonic spectrum "REL" corresponding to a value of $\nu_{anh}(OHs)$ based on the relaxed potential as described in the last sections of this work. This calculation leads to an intensity of about 500 km/mol for the OH stretching normal mode with frequency near 2421 $cm^{-1.}$
(40) Pulay, P.; Fogarasi, G.; Boggs, J. E. *J. Chem. Phys.* **1981**, *74*, 3999.
(41) Person, W. B.; Szczepaniak, K. Unpublished results, 2004−2005.